

# Single Perturbative Splitting Diagrams in Double Parton Scattering

---

Jonathan R. Gaunt<sup>a,b</sup>

<sup>a</sup>*Cavendish Laboratory, University of Cambridge, J.J. Thomson Avenue, Cambridge CB3 0HE, U.K.*

<sup>b</sup>*Deutsches Elektronen-Synchrotron DESY, 22603 Hamburg, Germany*

*E-mail:* [gaunt@hep.phy.cam.ac.uk](mailto:gaunt@hep.phy.cam.ac.uk)

**ABSTRACT:** We present a detailed study of a specific class of graph that can potentially contribute to the proton-proton double parton scattering (DPS) cross section. These are the ‘2v1’ or ‘single perturbative splitting’ graphs, in which two ‘nonperturbatively generated’ ladders interact with two ladders that have been generated via a perturbative  $1 \rightarrow 2$  branching process. Using a detailed calculation, we confirm the result written down originally by Ryskin and Snigirev – namely, that the 2v1 graphs in which the two nonperturbatively generated ladders do not interact with one another do contribute to the leading order proton-proton DPS cross section, albeit with a different geometrical prefactor to the one that applies to the ‘2v2’/‘zero perturbative splitting’ graphs. We then show that 2v1 graphs in which the ‘nonperturbatively generated’ ladders exchange partons with one another also contribute to the leading order proton-proton DPS cross section, provided that this ‘crosstalk’ occurs at a lower scale than the  $1 \rightarrow 2$  branching on the other side of the graph. Due to the preference in the 2v1 graphs for the  $x$  value at which the branching occurs, and crosstalk ceases, to be very much larger than the  $x$  values at the hard scale, the effect of crosstalk interactions is likely to be a decrease in the 2v1 cross section except at exceedingly small  $x$  values ( $\lesssim 10^{-6}$ ). At moderate  $x$  values  $\simeq 10^{-3} - 10^{-2}$ , the  $x$  value at the splitting is in the region  $\simeq 10^{-1}$  where PDFs do not change much with scale, and the effect of crosstalk interactions is likely to be small. We give an explicit formula for the contribution from the 2v1 graphs to the DPS cross section, and combine this with a suggestion that we made in a previous publication, that the ‘double perturbative splitting’/‘1v1’ graphs should be completely removed from the DPS cross section, to obtain a formula for the DPS cross section. It is pointed out that there are two potentially concerning features in this equation, that might indicate that our prescription for handling the 1v1 graphs is not quite correct.

**KEYWORDS:** QCD, Hadronic Colliders

---

## Contents

<b>1</b>	<b>Introduction</b>	<b>1</b>
<b>2</b>	<b>‘Two versus One’ Contributions to the DPS Cross Section</b>	<b>5</b>
<b>3</b>	<b>Crosstalk between Ladders in the 2v1 Contribution</b>	<b>15</b>
<b>4</b>	<b>The Total Cross Section for Double Parton Scattering</b>	<b>25</b>
<b>5</b>	<b>Conclusions</b>	<b>27</b>

---

## 1 Introduction

We define double parton scattering (DPS) as the process in which two pairs of partons participate in hard interactions in a single proton-proton (p-p) collision. This process is formally suppressed relative to the usual single parton scattering (SPS) mechanism by  $\Lambda^2/Q^2$ , where  $Q^2$  is the scale of the hard scattering(s) involved, and  $\Lambda^2$  is the scale of nonperturbative physics. However, DPS can contribute important backgrounds to SPS processes that are suppressed by small or multiple coupling constants, such as Higgs or new physics signals [1–4]. It is also an interesting process to study in its own right, as it reveals novel information concerning correlations between partons in the proton. For any final state  $AB$  which can potentially have been produced via two independent scatterings yielding  $A$  and  $B$ , there is a region of final state phase space in which the DPS production mechanism is competitive with the SPS one – namely, the region in which the transverse momenta of  $A$  and  $B$  are small [5, 6]. This fact offers some scope to study DPS in detail – indeed it has been used in past experimental extractions of DPS [7–12]. Finally, the rate of DPS relative to SPS for a given final state  $AB$  increases with collider energy, as lower  $x$  values are probed where the population of partons is larger. This means that DPS will be more important at the LHC than at any previous collider. For these reasons, there has been a considerable increase in interest in the phenomenon of DPS in recent years from both the experimental and theoretical communities, and four international workshops have been organised on the theme [13–17].

If one assumes that the two hard processes  $A$  and  $B$  may be factorised, then the total cross section for the process  $pp \rightarrow AB + X$  via double parton scattering should be of the

following form:

$$\begin{aligned}
\sigma_{(A,B)}^D &\propto \sum_{i,j,k,l} \int \frac{d^2\mathbf{r}}{(2\pi)^2} \prod_{a=1}^4 dx_a \Gamma_{ij}(x_1, x_2, \mathbf{r}; Q_A^2, Q_B^2) \Gamma_{kl}(x_3, x_4, -\mathbf{r}; Q_A^2, Q_B^2) \\
&\quad \times \hat{\sigma}_{ik \rightarrow A}(\hat{s} = x_1 x_3 s) \hat{\sigma}_{jl \rightarrow B}(\hat{s} = x_2 x_4 s) \\
&\propto \sum_{i,j,k,l} \int d^2\mathbf{b} \prod_{a=1}^4 dx_a \Gamma_{ij}(x_1, x_2, \mathbf{b}; Q_A^2, Q_B^2) \Gamma_{kl}(x_3, x_4, \mathbf{b}; Q_A^2, Q_B^2) \\
&\quad \times \hat{\sigma}_{ik \rightarrow A}(\hat{s} = x_1 x_3 s) \hat{\sigma}_{jl \rightarrow B}(\hat{s} = x_2 x_4 s)
\end{aligned} \tag{1.1}$$

The  $\hat{\sigma}$  symbols represent parton-level cross sections.  $\Gamma_{ij}(x_1, x_2, \mathbf{b}; Q_A^2, Q_B^2)$  is the impact-parameter space two-parton GPD ( $\mathbf{b}$ -space 2pGPD), whilst  $\Gamma_{ij}(x_1, x_2, \mathbf{r}; Q_A^2, Q_B^2)$  is the transverse momentum space 2pGPD ( $\mathbf{r}$ -space 2pGPD).  $\Gamma_{ij}(x_1, x_2, \mathbf{b}; Q_A^2, Q_B^2)$  has a probability interpretation as the probability to find a pair of quarks in the proton with flavours  $ij$ , momentum fractions  $x_1 x_2$ , and separated by impact parameter  $\mathbf{b}$ , at scales  $Q_A$  and  $Q_B$  respectively [5, 6, 18]. The  $\mathbf{r}$ -space 2pGPD is the Fourier transform of this with respect to  $\mathbf{b}$ , and has no probability interpretation.  $\mathbf{r}$  is related to the transverse momentum imbalance of one of the partons emerging from the proton between amplitude and conjugate (for more detail, see Section 2 of [5]).

Since the experimental extraction of DPS relies on the fact that the DPS cross section differential in the transverse momenta of  $A$  and  $B$ ,  $\mathbf{q}_A$  and  $\mathbf{q}_B$ , is strongly peaked at small  $\mathbf{q}_A$  and  $\mathbf{q}_B$ , it is perhaps the DPS cross section differential in  $\mathbf{q}_A$  and  $\mathbf{q}_B$  rather than the total cross section that is more relevant for making experimentally testable predictions [5, 6, 18, 19]. In the region of  $\mathbf{q}_A, \mathbf{q}_B$  of interest (i.e.  $\mathbf{q}_A^2, \mathbf{q}_B^2 \ll Q_A^2, Q_B^2$ ) this quantity is described in terms of transverse momentum dependent 2pGPDs (TMD 2pGPDs), rather than the collinear 2pGPDs appearing in (1.1). On the other hand, it is expected that for  $\Lambda^2 \ll \mathbf{q}_A^2, \mathbf{q}_B^2 \ll Q_A^2, Q_B^2$  the TMD 2pGPD should be expressible in terms of the collinear 2pGPD and a perturbatively calculable piece [5, 6]. In that case there is a ‘collinear part’ of the differential cross section whose structure closely resembles the total cross section formula (1.1). Knowledge of how the total DPS cross section is to be treated should be helpful in establishing the correct way to treat this collinear part. It is with this ultimate purpose in mind that we continue to discuss only the total cross section for DPS in the remainder of the paper.

There are several classes of graph that can potentially contribute to the leading order (LO) p-p DPS cross section (we restrict our attention to leading order, or leading logarithmic accuracy, in this paper). These are sketched in figure 1. Note that the partons emerging from the grey proton blobs in the figure are nonperturbatively generated partons – i.e. ones existing at a low scale  $\sim \Lambda_{QCD}$  – and that we’ve taken all the hard processes in the figure to be the production of an electroweak gauge boson with positive invariant mass (denoted by a wiggly line). We’ll refer to the different classes of graph (a), (b), and (c) as 2v2, 2v1 and 1v1 graphs respectively, for obvious reasons.

In the paper [20], we carefully examined graphs of the 1v1 type. We found that the treatment of these graphs by a long-established framework for calculating the p-p DPS

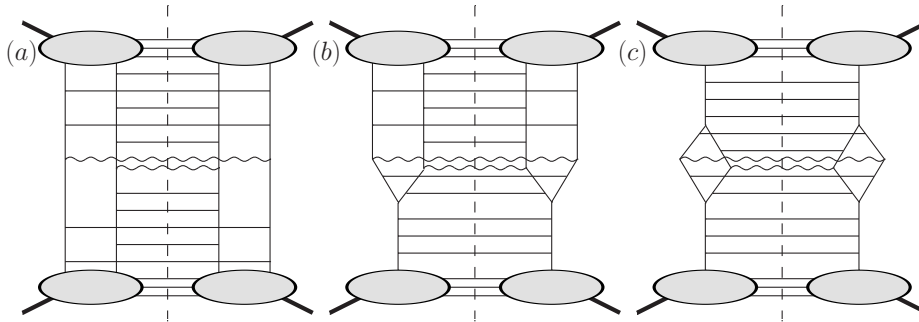


**Figure 1.** Some types of graph that can potentially contribute to the DPS cross section.

cross section [21–23] was unsatisfactory, and suggested that no part of these graphs should be included as part of the leading order p-p DPS cross section. Since then, this suggestion has also been made in a number of other papers [19, 24].

In light of this discovery, a careful re-analysis of other classes of graph that can potentially contribute to the LO DPS cross section would seem appropriate. In this paper we will pay particular attention to the 2v1 graphs in which there is only a single perturbative splitting, such as that drawn in figure 1(b) (we’ll also discuss to a certain extent 2v2 graphs such as 1(a) in which there are no perturbative splittings, although it should be reasonably clear that these should be included in the LO DPS cross section).

In section 2, we will begin to address the issue of whether contributions from the 2v1 graphs should be included in the LO DPS cross section, and what form these contributions should take. We’ll do this using a similar strategy as we employed for the 1v1 graphs in the paper [20]. That is, we’ll take a 2v1 graph with the simplest possible structure (i.e. the structure of figure 2) and see whether there is a ‘natural’ part of the cross section expression for it that is proportional to  $1/R_p^2$  ( $R_p =$  proton radius), and also contains a large logarithm associated with the  $1 \rightarrow 2$  splitting. The large logarithm should be associated with transverse momenta of the partons emerging from the  $1 \rightarrow 2$  splitting being  $\ll Q^2$  (where we take  $Q_A^2 = Q_B^2 \equiv Q^2$  for simplicity). If there is such a structure in the 2v1 graph, then this part of this graph should be included in the LO DPS cross section. Furthermore, if there is a  $\log(Q^2/\Lambda^2)/R_p^2$  structure in the simplest 2v1 diagram, then we expect there to be a  $\log(Q^2/\Lambda^2)^n/R_p^2$  piece in the more general 2v1 diagram of figure 1(b) that should also be included in the LO DPS cross section. This will be associated with the branchings in the diagram being strongly ordered in transverse momentum. From the structure of the contribution to the LO DPS cross section coming from the simplest 2v1 diagram, we’ll be able to write down a resummed expression for the contribution to the LO DPS cross section coming from 2v1 diagrams with the structure of figure 1(b).

The results that we obtain in section 2 have in fact already been written down in the papers [19, 24–26], and one can view the content of that section as a more detailed re-derivation of some of the results in those papers. In section 3, we will however establish a further result with regard to the contribution of 2v1 graphs to the LO DPS cross section. We will discover that the final formula that we obtained in section 2 is incom-

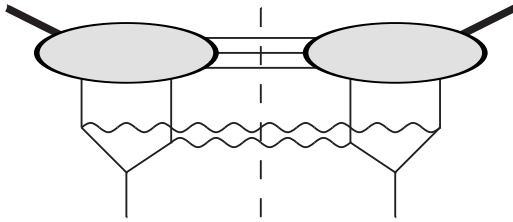


**Figure 2.** The simplest structure possible for the 2v1 graph.

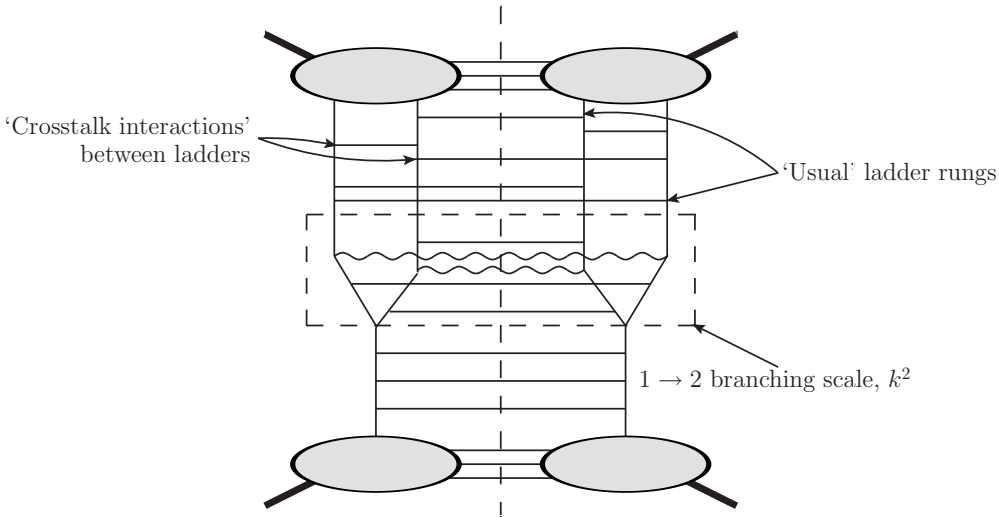


**Figure 3.** Generic 2v1 diagram including ‘crosstalk’ that we argue contributes to the 2v1 DPS cross section at the leading logarithmic level.

plete, and that there are further diagrams of the 2v1 type that contribute to the LO DPS cross section. These diagrams involve non-diagonal crosstalk interactions between the two nonperturbatively generated parton ladders, at scales lower than the perturbative  $1 \rightarrow 2$  ladder branching on the other side – an example diagram of this type is sketched in figure 3 (note that there are no such crosstalk interactions in figure 1(b)). This result is again established by analysis of the simplest Feynman graphs of the appropriate type. In section 3 we’ll also discuss in detail the issue of colour in relation to the crosstalk interactions, and make some comments with regard to the potential numerical impact of the crosstalk interactions on the 2v1 DPS cross section.

In section 4, we combine the results from sections 2 and 3 with our suggestion from [20] with regards to the 1v1 graphs, to give a suggested expression for the LO cross section for DPS. We do however point out two potentially concerning features in this equation that may indicate that the suggestion of [20] to completely remove the 1v1 graphs from the DPS cross section is not quite the correct prescription.

## 2 ‘Two versus One’ Contributions to the DPS Cross Section

In this section, we show explicitly that for a 2v1 diagram with the structure of figure 2, there is a part of the cross section expression that contains a DGLAP-type large logarithm and a factor of order  $1/R_p^2$ , which should be considered as part of the LO DPS cross section. We present details of the calculation only for the particular flavour-diagonal contribution to the  $gp \rightarrow gq\bar{q} + X \rightarrow \gamma^*\gamma^* + X$  process presented in figure 4(a), where the two off-shell photons both have a positive invariant mass. However, the general method outlined below can be applied to any diagram of the appropriate structure, and will always give a large logarithm provided that the corresponding process is allowed in the collinear limit (apart from issues of  $J_z$  nonconservation at the splitting vertex).

In the calculation of the cross section for figure 4(a), we will have to include a wavefunction factor or hadronic amplitude  $\varphi$  to find two nonperturbatively generated partons in the proton, at the amplitude level in the calculation. It would be inappropriate to try and calculate a 2v1 cross section in a naive ‘fully parton-level’ way omitting the proton at the top of the diagram because then one would have three particles in the initial state (whereas the standard framework for calculating a cross section requires two particles in the initial state). Furthermore, by deleting the proton at the top of the diagram one would then be neglecting the important fact that the two partons on this side are tied together in the same proton (as was pointed out in [19]). The use of proton wavefunctions or hadronic amplitudes in the calculation of DPS-type graphs was discussed long ago in [27], and has been discussed more recently in [6, 19]. We utilise the approach and notation of [27] in our work. That is, we assign a wavefunction factor  $\varphi$  to the  $p \rightarrow q\bar{q}X$  vertex that is assumed to be strongly damped for values of the parton transverse momentum and virtuality larger than the hadronic scale  $\Lambda \sim 1/R_P$ . In our case the factor  $\varphi$  is a matrix in spinor space, and also carries a label  $\chi$  that describes the spins of all of the particles in  $X$ .

In the following we will take a number of steps to simplify the calculation as much as possible. First, we will largely ignore considerations of colour, and will suppress colour indices, factors and sums where they appear, in order to avoid the proliferation of too many indices. Second, we will take the four-momenta squared of the two off-shell photons to be the same, and refer to this common four-momentum squared as  $Q^2$ . Finally, we will take the colliding protons to be unpolarised, as is the case for the colliding protons at the LHC.

As in [20], we apply a Sudakov decomposition to all four-vectors used – that is, we write an arbitrary four-vector  $V$  in terms of two lightlike vectors  $p \equiv \frac{1}{\sqrt{2}}(1, 0, 0, 1)$  and  $n \equiv \frac{1}{\sqrt{2}}(1, 0, 0, -1)$  and a transverse part denoted as  $\mathbf{V}$ :

$$V = V^+p + V^-n + \mathbf{V} \tag{2.1}$$

Rather than proceeding to calculate the cross section contribution from figure 4(a) directly, we instead begin by calculating the cross section contribution  $\sigma_{2v2}$  associated with the Feynman diagram in figure 4(b). In this diagram, two nonperturbatively generated quark-antiquark pairs produced by colliding protons interact via two separate  $q\bar{q} \rightarrow \gamma^*$  hard processes. We should be able to express the cross section of this process in terms of

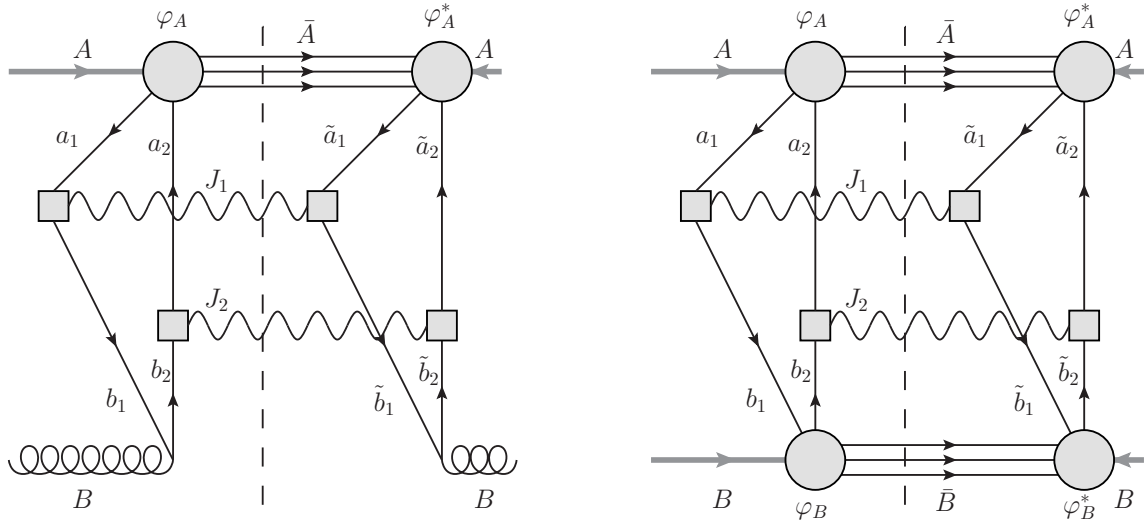


**Figure 4.** (a) An example of a ‘2v1’ DPS-type scattering diagram. (b) An example of a ‘2v2’ DPS-type scattering diagram. The thick grey lines are protons, whilst the grey circles are proton vertices. The labels on the lines correspond to the four momenta of those lines.

‘nonperturbatively generated parton pair’  $\mathbf{r}$ -space 2pGPDs  $\Gamma(x_1, x_2; \Delta)$  and hard subprocess cross sections  $\hat{\sigma}$  as follows:

$$\begin{aligned} \sigma_{2v2}(s) &= \int dx_1 dx_2 dy_1 dy_2 \hat{\sigma}_{q\bar{q} \rightarrow \gamma^*}(\hat{s} = x_1 y_1 s) \hat{\sigma}_{q\bar{q} \rightarrow \gamma^*}(\hat{s} = x_2 y_2 s) \\ &\times \int \frac{d^2 \Delta}{(2\pi)^2} \Gamma_p(x_1, x_2; \Delta) \Gamma_p(y_1, y_2; -\Delta) \end{aligned} \quad (2.2)$$

Helicity labels are omitted in the above schematic expression, but they will be included in the full calculation below. By using the fact that the expression for the cross section must end up in this form, we can establish the connection between the vertex factor  $\varphi$  and the ‘nonperturbatively generated parton pair’  $\mathbf{r}$ -space 2pGPD  $\Gamma$ . We shall need to make use of this relationship when we come to study figure 4(a).

Note that a calculation of  $\sigma_{2v2}$  has already been performed by Paver and Treleani in [27] for the case of spinless partons, and by Mekhfi [28] and Diehl, Ostermeier and Schafer [5, 6] for the case of partons with spin. We follow closely the approach of Paver and Treleani, and our calculation of  $\sigma_{2v2}$  can be considered as a brief review of the method in [27].

We will neglect the proton mass with respect to the total centre of mass energy  $\sqrt{s}$  and work in a frame in which  $A$  is proportional to  $p$ , whilst  $B$  is proportional to  $n$ ,  $A = A^+ p, B = B^- n$ . One can directly write down the following expression for the cross section contribution from figure 4(b),  $\sigma_{2v2}(s)$ :

$$\begin{aligned} \sigma_{2v2}(s) &= \frac{1}{2(2\pi)^{10} s} \sum_{\chi\gamma} \int d^4 \bar{A} d^4 \bar{B} d^4 J_1 d^4 J_2 \delta^{(4)}(\bar{A} + \bar{B} + J_1 + J_2 - A - B) \delta(J_1^2 - Q^2) \\ &\times \delta(J_2^2 - Q^2) \mathcal{M}^{\chi\gamma\mu_1\mu_2}(A, B; \bar{A}, \bar{B}, J_1, J_2) \mathcal{M}^{\chi\gamma\mu_1\mu_2}(A, B; \bar{A}, \bar{B}, J_1, J_2)^* \end{aligned} \quad (2.3)$$

where:

$$\begin{aligned} \mathcal{M}^{\chi\gamma\mu_1\mu_2}(A, B; \bar{A}, \bar{B}, J_1, J_2) & \quad (2.4) \\ & \equiv \int \frac{d^4 a_1}{(2\pi)^4} \frac{\text{Tr} [T^{\mu_1}(J_1) \not{a}_1 \varphi_p^\chi(a_1, a_2, \bar{A}) \not{a}_2 T^{\mu_2}(J_2) \not{b}_2 \varphi_p^\gamma(b_2, b_1, \bar{B}) \not{b}_1]}{D(a_1)D(a_2)D(b_1)D(b_2)}, \end{aligned}$$

$$D(a) \equiv a^2 + i\epsilon, \quad T^{\mu_1}(J_1) \equiv ieQ_q \not{e}_{\mu_1}^*(J_1) \quad (2.5)$$

$$a_2 \equiv A - \bar{A} - a_1 \quad b_1 \equiv J_1 - a_1 \quad b_2 \equiv B - \bar{B} + a_1 - J_1 \quad (2.6)$$

The vertex factors  $\varphi$  ensure that the quark and antiquark lines with momenta  $a_i$  and  $b_i$  have small virtuality. Given that this is the case, we can rewrite the slashed vectors in (2.4) as sums over outer products of particle or antiparticle spinors (as appropriate), using the completeness relations. Then we have:

$$\begin{aligned} \mathcal{M}^{\chi\gamma\mu_1\mu_2}(A, B; \bar{A}, \bar{B}, J_1, J_2) & \quad (2.7) \\ & \simeq \int \frac{d^4 a_1}{(2\pi)^4} \sum_{s_i t_i} \mathcal{M}_{q\bar{q} \rightarrow \gamma^*}^{s_1 t_1; \mu_1}(a_1 b_1 \rightarrow J_1) \mathcal{M}_{q\bar{q} \rightarrow \gamma^*}^{s_2 t_2; \mu_2}(a_2 b_2 \rightarrow J_2) \\ & \quad \times \left[ \frac{\bar{u}^{s_1}(a_1) \varphi_p^\chi(a_1, a_2, \bar{A}) v^{s_2}(a_2)}{D(a_1)D(a_2)} \right] \left[ \frac{\bar{u}^{t_2}(b_2) \varphi_p^\gamma(b_2, b_1, \bar{B}) v^{t_1}(b_1)}{D(b_1)D(b_2)} \right] \end{aligned}$$

The  $s_i$  and  $t_i$  are quark or antiquark helicity labels, and the  $\mathcal{M}_{q\bar{q} \rightarrow \gamma^*}$  factors are ‘hard’  $q\bar{q} \rightarrow \gamma^*$  matrix elements. The hard matrix elements should be evaluated with initial state partons having small (i.e. hadron scale) transverse momenta and off-shellness – however, we make the approximation in the matrix elements that the initial-state partons are on-shell and collinear, which only corresponds to a small relative error  $\mathcal{O}(\Lambda^2/Q^2) \ll 1$ .

Consider now the integrations over the longitudinal parts of  $a_1$  – i.e.  $a_1^+$  and  $a_1^-$ . It is not hard to show that the integration over  $a_1^-$  is restricted to values of order  $\Lambda^2/Q$  by the vertex factor  $\varphi(a_1, a_2, \bar{A})$ , whilst  $\varphi(b_1, b_2, \bar{B})$ ,  $D(b_i)$ , and the  $\mathcal{M}_{q\bar{q} \rightarrow \gamma^*}$  are practically constant in this range (and approximately equal to their values with  $a_1^-$  set to zero). Similarly, the integration over  $a_1^+$  is restricted to values differing from  $J_1^+$  by  $\sim \Lambda^2/Q$  by the vertex factor  $\varphi(b_1, b_2, \bar{B})$ , with  $\varphi(a_1, a_2, \bar{A})$ ,  $D(a_i)$  and the  $\mathcal{M}_{q\bar{q} \rightarrow \gamma^*}$  being approximately constant and equal to their values at  $a_1^+ = J_1^+$  in this range. This allows us to write:

$$\begin{aligned} \mathcal{M}^{\chi\gamma\mu_1\mu_2}(A, B; \bar{A}, \bar{B}, J_1, J_2) & \simeq \sum_{s_i t_i} \mathcal{M}_{q\bar{q} \rightarrow \gamma^*}^{s_1 t_1; \mu_1}(J_1^+ p, J_1^- n \rightarrow J_1) \quad (2.8) \\ & \times \mathcal{M}_{q\bar{q} \rightarrow \gamma^*}^{s_2 t_2; \mu_2}(J_2^+ p, J_2^- n \rightarrow J_2) \int \frac{d^2 \mathbf{a}_1}{(2\pi)^2} \left[ \int \frac{da_1^-}{2\pi} \frac{\bar{u}^{s_1}(a_1) \varphi_p^\chi(a_1, a_2, \bar{A}) v^{s_2}(a_2)}{D(a_1)D(a_2)} \right]_{a_1^+ = J_1^+} \\ & \times \left[ \int \frac{db_1^+}{2\pi} \frac{\bar{u}^{t_2}(b_2) \varphi_p^\gamma(b_2, b_1, \bar{B}) v^{t_1}(b_1)}{D(b_1)D(b_2)} \right]_{b_1^- = J_1^-} \end{aligned}$$

Define:

$$\psi_{p; q\bar{q}}^{s_1 s_2 \chi}(a_1^+, a_2^+, \mathbf{a}_1, \mathbf{a}_2, \bar{A}^-) \equiv - \int \frac{da_1^-}{2\pi} \frac{\bar{u}^{s_1}(a_1) \varphi_p^\chi(a_1, a_2, \bar{A}) v^{s_2}(a_2)}{D(a_1)D(a_2)} \quad (2.9)$$

Then we can write  $\mathcal{M}^{\chi\gamma\mu_1\mu_2}(A, B; \bar{A}, \bar{B}, J_1, J_2)$  in a more compact form:

$$\begin{aligned} & \mathcal{M}^{\chi\gamma\mu_1\mu_2}(A, B; \bar{A}, \bar{B}, J_1, J_2) \\ & \simeq \sum_{s_i \tilde{t}_i} \mathcal{M}_{q\bar{q} \rightarrow \gamma^*}^{s_1 t_1; \mu_1}(J_1^+ p, J_1^- n \rightarrow J_1) \mathcal{M}_{q\bar{q} \rightarrow \gamma^*}^{s_2 t_2; \mu_2}(J_2^+ p, J_2^- n \rightarrow J_2) \\ & \quad \times \int \frac{d^2 \mathbf{a}_1}{(2\pi)^2} \psi_{p; q\bar{q}}^{s_1 s_2 \chi}(J_1^+, J_2^+, \mathbf{a}_1, \mathbf{a}_2, \bar{A}^-) \psi_{p; q\bar{q}}^{t_2 t_1 \gamma}(J_2^-, J_1^-, \mathbf{b}_2, \mathbf{b}_1, \bar{B}^+) \end{aligned} \quad (2.10)$$

We now insert (2.10) into (2.3), and make use of the following relation in the resulting expression:

$$\begin{aligned} & \mathcal{M}_{q\bar{q} \rightarrow \gamma^*}^{s_1 t_1; \mu_1}(J_1^+ p, J_1^- n \rightarrow J_1) \mathcal{M}_{q\bar{q} \rightarrow \gamma^*}^{* \tilde{s}_1 \tilde{t}_1; \mu_1}(J_1^+ p, J_1^- n \rightarrow J_1) (2\pi) \delta(J_1^2 - Q^2) \\ & = \hat{\sigma}_{q\bar{q} \rightarrow \gamma^*}^{s_1, t_1; \tilde{s}_1, \tilde{t}_1; \mu_1}(\hat{s} = 2J_1^+ J_1^-) 4J_1^+ J_1^- \end{aligned} \quad (2.11)$$

$\hat{\sigma}_{q\bar{q} \rightarrow \gamma^*}^{s_1, t_1; \tilde{s}_1, \tilde{t}_1; \mu_1}$  is the  $q\bar{q} \rightarrow \gamma^*$  ‘cross section’ with  $q, \bar{q}, \gamma^*$  helicities  $s_1, t_1, \mu_1$  in the matrix element, and  $\tilde{s}_1, \tilde{t}_1, \mu_1$  in the conjugate matrix element (note that if  $s_1 \neq \tilde{s}_1$  and/or  $t_1 \neq \tilde{t}_1$  this is not a cross section in the strict sense).  $\hat{\sigma}_{q\bar{q} \rightarrow \gamma^*}^{s_1, t_1; \tilde{s}_1, \tilde{t}_1; \mu_1}$  is related to the spin-averaged  $q\bar{q} \rightarrow \gamma^*$  cross section  $\hat{\sigma}_{q\bar{q} \rightarrow \gamma^*}$  by:

$$\hat{\sigma}_{q\bar{q} \rightarrow \gamma^*}^{s_1, t_1; \tilde{s}_1, \tilde{t}_1; \mu_1} = 2\hat{\sigma}_{q\bar{q} \rightarrow \gamma^*} \delta_{s_1, -t_1} \delta_{\tilde{s}_1, -\tilde{t}_1} \quad (2.12)$$

The result of inserting (2.10) into (2.3) is:

$$\begin{aligned} \sigma_{2v2}(s) &= \frac{1}{2(2\pi)^{12} s} \sum_{s_i t_i \tilde{s}_i \tilde{t}_i \chi \gamma} \int d^4 \bar{A} d^4 \bar{B} d^4 J_1 \hat{\sigma}_{q\bar{q} \rightarrow \gamma^*}^{s_1, t_1; \tilde{s}_1, \tilde{t}_1; \mu_1}(\hat{s} = 2J_1^+ J_1^-) 4J_1^+ J_1^- \\ & \quad \times \hat{\sigma}_{q\bar{q} \rightarrow \gamma^*}^{s_2, t_2; \tilde{s}_2, \tilde{t}_2; \mu_2}(\hat{s} = 2J_2^+ J_2^-) 4J_2^+ J_2^- \int \frac{d^2 \mathbf{a}_1}{(2\pi)^2} \frac{d^2 \tilde{\mathbf{a}}_1}{(2\pi)^2} \psi_{p; q\bar{q}}^{s_1 s_2 \chi}(J_1^+, J_2^+, \mathbf{a}_1, \mathbf{a}_2, \bar{A}^-) \\ & \quad \times \psi_{p; q\bar{q}}^{t_2 t_1 \gamma}(J_2^-, J_1^-, \mathbf{b}_2, \mathbf{b}_1, \bar{B}^+) \psi_{p; q\bar{q}}^{* \tilde{s}_1 \tilde{s}_2 \chi}(J_1^+, J_2^+, \tilde{\mathbf{a}}_1, \tilde{\mathbf{a}}_2, \bar{A}^-) \psi_{p; q\bar{q}}^{* \tilde{t}_2 \tilde{t}_1 \gamma}(J_2^-, J_1^-, \tilde{\mathbf{b}}_2, \tilde{\mathbf{b}}_1, \bar{B}^+) \\ & = \frac{1}{4(2\pi)^{16} A^{+2} B^{-2}} \sum_{s_i t_i s'_i t'_i} \int d\bar{A}^+ d\bar{B}^- dJ_1^+ dJ_1^- \hat{\sigma}_{q\bar{q} \rightarrow \gamma^*}^{s_1, t_1; \tilde{s}_1, \tilde{t}_1; \mu_1}(\hat{s} = 2J_1^+ J_1^-) \\ & \quad \times \hat{\sigma}_{q\bar{q} \rightarrow \gamma^*}^{s_2, t_2; \tilde{s}_2, \tilde{t}_2; \mu_2}(\hat{s} = 2J_2^+ J_2^-) \int d^2 \mathbf{a}_1 d^2 \mathbf{b}_1 d^2 \Delta d^2 \bar{A} d\bar{A}^- d^2 \bar{B} d\bar{B}^+ \\ & \quad \times \sum_{\chi} \psi_{p; q\bar{q}}^{s_1 s_2 \chi}(J_1^+, J_2^+, \mathbf{a}_1, \mathbf{a}_2, \bar{A}^-) \psi_{p; q\bar{q}}^{* \tilde{s}_1 \tilde{s}_2 \chi}(J_1^+, J_2^+, \mathbf{a}_1 + \Delta, \mathbf{a}_2 - \Delta, \bar{A}^-) 4J_1^+ J_2^+ A^+ \\ & \quad \times \sum_{\gamma} \psi_{p; q\bar{q}}^{t_2 t_1 \gamma}(J_2^-, J_1^-, \mathbf{b}_2, \mathbf{b}_1, \bar{B}^+) \psi_{p; q\bar{q}}^{* \tilde{t}_2 \tilde{t}_1 \gamma}(J_2^-, J_1^-, \mathbf{b}_2 + \Delta, \mathbf{b}_1 - \Delta, \bar{B}^+) 4J_1^- J_2^- B^- \end{aligned} \quad (2.13)$$

In the second line of (2.13), we have introduced the transverse variable  $\Delta$  via  $\mathbf{a}_1 = \tilde{\mathbf{a}}_1 + \Delta$ , and converted the integral over  $\mathbf{J}_1$  to an integral over  $\mathbf{b}_1$  using  $\mathbf{a}_1 + \mathbf{b}_1 = \mathbf{J}_1$ . We have also made use of the fact that  $s = 2A^+ B^-$ . Let us define the ‘nonperturbatively generated parton pair’  $\mathbf{r}$ -space 2pGPD according to:

$$\begin{aligned} \Gamma_{p; q\bar{q}}^{s_1 s_2, \tilde{s}_1 \tilde{s}_2} \left( \frac{J_1^+}{A^+}, \frac{J_2^+}{A^+}; \Delta \right) & \equiv \frac{2}{(2\pi)^7} \sum_{\chi} \int d\bar{A}^- d^2 \bar{A} d^2 \mathbf{a}_1 \psi_{p; q\bar{q}}^{s_1 s_2 \chi}(J_1^+, J_2^+, \mathbf{a}_1, \mathbf{a}_2, \bar{A}^-, \bar{A}) \\ & \quad \times \psi_{p; q\bar{q}}^{* \tilde{s}_1 \tilde{s}_2 \chi}(J_1^+, J_2^+, \mathbf{a}_1 + \Delta, \mathbf{a}_2 - \Delta, \bar{A}^-, \bar{A}) J_1^+ J_2^+ A^+ \end{aligned} \quad (2.14)$$

We also introduce the following scaling variables:

$$x_1 \equiv J_1^+/A^+ \quad x_2 \equiv J_2^+/A^+ \quad y_1 \equiv J_1^-/B^- \quad y_2 \equiv J_2^-/B^- \quad (2.15)$$

Changing variables in (2.13) to the scaling variables, replacing appropriate combinations of  $\psi$ s by  $\Gamma$ s according to (2.14), and using the obvious relation  $\Gamma_{p;\bar{q}q}^{s_1 s_2, \tilde{s}_1 \tilde{s}_2}(x_1, x_2; \mathbf{\Delta}) = \Gamma_{p;\bar{q}q}^{s_2 s_1, \tilde{s}_2 \tilde{s}_1}(x_2, x_1; -\mathbf{\Delta})$ , we finally obtain:

$$\begin{aligned} \sigma_{2v2}(s) &= \sum_{s_i \tilde{t}_i \tilde{t}_i} \int dx_1 dx_2 dy_1 dy_2 \hat{\sigma}_{q\bar{q} \rightarrow \gamma^*}^{s_1, t_1; \tilde{s}_1, \tilde{t}_1; \mu_1}(\hat{s} = x_1 y_1 s) \hat{\sigma}_{q\bar{q} \rightarrow \gamma^*}^{s_2, t_2; \tilde{s}_2, \tilde{t}_2; \mu_2}(\hat{s} = x_2 y_2 s) \quad (2.16) \\ &\times \int \frac{d^2 \mathbf{\Delta}}{(2\pi)^2} \Gamma_{p;\bar{q}q}^{s_1 s_2, \tilde{s}_1 \tilde{s}_2}(x_1, x_2; \mathbf{\Delta}) \Gamma_{p;\bar{q}q}^{t_1 t_2, \tilde{t}_1 \tilde{t}_2}(y_1, y_2; -\mathbf{\Delta}) \end{aligned}$$

The cross section is of the anticipated form (2.2). The most important result of this preliminary calculation is the definition of the ‘nonperturbatively generated parton pair’  $\mathbf{r}$ -space 2pGPD (2.14), which we shall make use of later.

The calculation of the cross section contribution associated with figure 4(a),  $\sigma_{2v1}(s)$ , proceeds in a very similar manner to the calculation of  $\sigma_{2v2}(s)$ . Once again we work in a frame in which  $A = A^+p$  and  $B = B^+n$ . We can directly write down the following expression for the cross section:

$$\begin{aligned} \sigma_{2v1}(s) &= \frac{1}{2(2\pi)^6 s} \sum_{\chi} \int d^4 \bar{A} d^4 J_1 d^4 J_2 \delta(J_1^2 - Q^2) \delta(J_2^2 - Q^2) \delta^{(4)}(\bar{A} + J_1 + J_2 - A - B) \\ &\times \mathcal{M}^{\lambda; \chi \mu_1 \mu_2}(A, B; \bar{A}, J_1, J_2) \mathcal{M}^{\lambda; \chi \mu_1 \mu_2}(A, B; \bar{A}, J_1, J_2)^* \end{aligned} \quad (2.17)$$

where:

$$\begin{aligned} \mathcal{M}^{\lambda; \chi \mu_1 \mu_2}(A, B; \bar{A}, J_1, J_2) & \quad (2.18) \\ &\equiv \int \frac{d^4 a_1}{(2\pi)^4} i^2 \text{Tr}(\not{a}_1 \varphi_p^\chi(a_1, a_2, \bar{A}) \not{a}_2 T^{\lambda; \mu_1 \mu_2}(a_2 a_1 B \rightarrow J_1 J_2)) / [D(a_1) D(a_2)], \end{aligned}$$

$$T^{\lambda; \mu_1 \mu_2}(a_2 a_1 B \rightarrow J_1 J_2) \equiv i^5 (e Q_q)^2 g_s \frac{\not{a}_2^* \not{J}_2 \not{b}_2 \not{a}_\lambda(B) \not{b}_1 \not{a}_1^*(J_1)}{D(b_1) D(b_2)} \quad (2.19)$$

The lines with momentum  $a_1$  are restricted to small virtuality by  $\varphi_A$ , so we can decompose the slashed  $a_i$  vectors in (2.18) into outer products of particle or antiparticle spinors:

$$\begin{aligned} \mathcal{M}^{\lambda; \chi \mu_1 \mu_2}(A, B; \bar{A}, J_1, J_2) & \quad (2.20) \\ &\simeq \sum_{s_i} \int \frac{d^4 a_1}{(2\pi)^4} \left[ -\frac{\bar{u}^{s_1}(a_1) \varphi_p^\chi(a_1, a_2, \bar{A}) v^{s_2}(a_2)}{D(a_1) D(a_2)} \right] \mathcal{M}^{s_2 s_1 \lambda; \mu_1 \mu_2}(a_2 a_1 B \rightarrow J_1 J_2) \end{aligned}$$

$\mathcal{M}^{s_2 s_1 \lambda; \mu_1 \mu_2}(a_2 a_1 B \rightarrow J_1 J_2)$  is the matrix element for  $q\bar{q}g \rightarrow \gamma^* \gamma^*$  with initial quark and antiquark having small transverse momentum and virtuality.

For reasons similar to those leading to equation (2.8), we can move the  $a_1^-$  integration such that it only acts on the part of (2.20) in square brackets, and set  $a_1^- = 0$  in the rest of the integrand. Provided that  $\mathbf{J}_1^2 \gg \Lambda^2$ , we can perform an analogous operation for the  $\mathbf{a}_1$  integration. The reason for this is that when  $\mathbf{J}_1^2 \gg \Lambda^2$ , the transverse momenta of the  $a_i$  lines (constrained to be of order  $\Lambda$  by  $\varphi_A$ ) are negligible compared to the transverse momenta of the  $b_i$  and  $J_i$  lines in  $\mathcal{M}^{s_2 s_1 \lambda; \mu_1 \mu_2}(a_2 a_1 B \rightarrow J_1 J_2)$ , so we make only a small error by setting  $\mathbf{a}_i$  to zero in this factor provided  $\mathbf{J}_1^2 \gg \Lambda^2$ . Applying these approximations:

$$\begin{aligned} \mathcal{M}^{\lambda; \chi \mu_1 \mu_2}(A, B; \bar{A}, J_1, J_2) & \quad (2.21) \\ & \simeq \sum_{s_i} \int \frac{da_1^+}{2\pi} \mathcal{M}^{s_2 s_1 \lambda; \mu_1 \mu_2}(a_2 a_1 B \rightarrow J_1 J_2)|_{a_1^- = 0, \mathbf{a}_1 = 0} \\ & \quad \times - \int \frac{d^2 \mathbf{a}_1}{(2\pi)^2} \frac{da_1^-}{2\pi} \frac{[\bar{u}^{s_1}(a_1) \varphi_p^X(a_1, a_2, \bar{A}) v^{s_2}(a_2)]}{D(a_1) D(a_2)} \end{aligned}$$

We identify the final factor in (2.21) as the integral of  $\psi_p$  over  $\mathbf{a}_1$ . Writing out the denominator factors in  $\mathcal{M}^{s_2 s_1 \lambda; \mu_1 \mu_2}(a_2 a_1 B \rightarrow J_1 J_2)$  explicitly we have:

$$\begin{aligned} \mathcal{M}^{\lambda; \chi \mu_1 \mu_2}(A, B; \bar{A}, J_1, J_2) & \quad (2.22) \\ & \simeq \sum_{s_i} \int \frac{da_1^+}{2\pi} \left[ \int d^2 \mathbf{a}_1 / (2\pi)^2 \psi_p^{s_1 s_2 \chi}(a_1^+, a_2^+, \mathbf{a}_1, \mathbf{a}_2, \bar{A}^-) \right] \\ & \quad \times \frac{\mathcal{T}^{s_2 s_1 \lambda; \mu_1 \mu_2}(a_2 a_1 B \rightarrow J_1 J_2)|_{a_1^- = 0, \mathbf{a}_1 = 0}}{[2(J_1^+ - a_1^+) J_1^- - \mathbf{J}_1^2 + i\epsilon][2(a_1^+ - J_1^+) J_2^- - \mathbf{J}_1^2 + i\epsilon]} \end{aligned}$$

where:

$$\mathcal{T}^{s_2 s_1 \lambda; \mu_1 \mu_2}(a_2 a_1 B \rightarrow J_1 J_2) \equiv i^5 g_s (eQ_q)^2 \bar{v}^{s_2}(a_2) \not{\epsilon}_{\mu_2}^* (J_2) \not{b}_2 \not{\epsilon}_\lambda (B) \not{b}_1 \not{\epsilon}_{\mu_1}^* (J_1) u^{s_1}(a_1) \quad (2.23)$$

Examination of the denominator factors in (2.21) reveals that the majority of the contribution to the  $a_1^+$  integration comes from the region  $a_1^+ \sim J_1^+$ . For this reason we can set  $a_1^+ = J_1^+$  in the numerator before evaluating the  $a_1^+$  integral using contour integration:

$$\begin{aligned} \mathcal{M}^{\lambda; \chi \mu_1 \mu_2}(A, B; \bar{A}, J_1, J_2) & \quad (2.24) \\ & \simeq \sum_{s_i} i \left[ \int d^2 \mathbf{a}_1 / (2\pi)^2 \psi_p^{s_1 s_2 \chi}(J_1^+, J_2^+, \mathbf{a}_1, \mathbf{a}_2, \bar{A}^-) \right] \\ & \quad \times \frac{\mathcal{T}^{s_2 s_1 \lambda; \mu_1 \mu_2}(a_2 a_1 B \rightarrow J_1 J_2)|_{a_1^- = 0, \mathbf{a}_1 = 0, a_1^+ = J_1^+}}{2(J_1^- + J_2^-) \mathbf{J}_1^2} \end{aligned}$$

We are interested in the behaviour of  $\mathcal{M}^{\lambda; \chi \mu_1 \mu_2}(A, B; \bar{A}, J_1, J_2)$  when  $\mathbf{J}_1^2 \ll Q^2$  (but still  $\gg \Lambda^2$ ) such that all of the internal particles have transverse momenta and virtualities much less than  $Q$ . In this limit we can use spinor completeness relations to split  $\mathcal{T}$  up into two  $q\bar{q} \rightarrow \gamma^*$  matrix elements and one  $g \rightarrow q\bar{q}$  matrix element, with the quark and antiquark having small transverse momenta and virtuality  $\mathcal{O}(|\mathbf{J}_1|)$  in each matrix element. The quark and antiquark transverse momenta and virtualities can be set to zero in the ‘hard’  $q\bar{q} \rightarrow \gamma^*$  matrix elements with only a small accompanying error  $\mathcal{O}(\mathbf{J}_1^2/Q^2)$ , but we

must keep the term proportional to  $\mathbf{J}_1$  in the  $g \rightarrow q\bar{q}$  matrix element as this vanishes in the limit  $\mathbf{J}_1 \rightarrow 0$ :

$$\begin{aligned} & \mathcal{M}^{\lambda;\chi\mu_1\mu_2}(A, B; \bar{A}, J_1, J_2) \tag{2.25} \\ & \simeq \sum_{s_i \tilde{t}_i} \frac{-i \left[ \int d^2 \mathbf{a}_1 / (2\pi)^2 \psi_p^{s_1 s_2 \chi}(a_1^+, a_2^+, \mathbf{a}_1, \mathbf{a}_2, \bar{A}^-) \right] \mathcal{M}_{g \rightarrow q\bar{q}}^{\lambda \rightarrow t_1 t_2}(B; J_1^- n + \mathbf{J}_1, J_2^- n + \mathbf{J}_2)}{2(J_1^- + J_2^-) \mathbf{J}_1^2} \\ & \quad \times \mathcal{M}_{q\bar{q} \rightarrow \gamma^*}^{t_1 s_1 \rightarrow \mu_1}(J_1^- n, J_1^+ p; J_1^- n + J_1^+ p) \mathcal{M}_{q\bar{q} \rightarrow \gamma^*}^{t_2 s_2 \rightarrow \mu_2}(J_2^- n, J_2^+ p; J_2^- n + J_2^+ p) \end{aligned}$$

Having inserted (2.25) into (2.17), we use (2.11) and the following connection between  $\mathcal{M}_{g \rightarrow q\bar{q}}$  and helicity-dependent unregularised splitting functions in the result [29]:

$$\begin{aligned} & \frac{J_1^- J_2^-}{(J_1^- + J_2^-)^2} \mathcal{M}_{g \rightarrow q\bar{q}}^{\lambda \rightarrow t_1 t_2}(B; J_1^- n + \mathbf{J}_1, J_2^- n + \mathbf{J}_2) \mathcal{M}_{g \rightarrow q\bar{q}}^{*\lambda \rightarrow \tilde{t}_1 \tilde{t}_2}(B; J_1^- n + \mathbf{J}_1, J_2^- n + \mathbf{J}_2) \tag{2.26} \\ & = 2g_s^2 P_{g \rightarrow q\bar{q}}^{\lambda \rightarrow t_2 t_1, \tilde{t}_2 \tilde{t}_1} \left( \frac{J_2^-}{J_1^- + J_2^-} \right) \mathbf{J}_1^2 \end{aligned}$$

This yields:

$$\begin{aligned} \sigma_{2v1}(s) & = \sum_{s_i \tilde{s}_i \tilde{t}_i \tilde{s}_i \chi} \frac{4}{(2\pi)^{12} s} \int d^4 \bar{A} d^4 J_1 \hat{\sigma}_{q\bar{q} \rightarrow \gamma^*}^{s_1, t_1; \tilde{s}_1, \tilde{t}_1; \mu_1}(\hat{s} = 2J_1^+ J_1^-) J_1^+ \hat{\sigma}_{q\bar{q} \rightarrow \gamma^*}^{s_2, t_2; \tilde{s}_2, \tilde{t}_2; \mu_2}(\hat{s} = 2J_2^+ J_2^-) J_2^+ \\ & \quad \times \left[ \int d^2 \mathbf{a}_1 \psi_p^{s_1 s_2 \chi}(J_1^+, J_2^+, \mathbf{a}_1, \mathbf{a}_2, \bar{A}^-) \right] \tag{2.27} \\ & \quad \times \left[ \int d^2 \mathbf{a}'_1 \psi_p^{*\tilde{s}_1 \tilde{s}_2 \chi}(J_1^+, J_2^+, \tilde{\mathbf{a}}_1, \tilde{\mathbf{a}}_2, \bar{A}^-) \right] g_s^2 P_{g \rightarrow q\bar{q}}^{\lambda \rightarrow t_2 t_1, \tilde{t}_2 \tilde{t}_1} \left( \frac{J_2^-}{J_1^- + J_2^-} \right) \frac{1}{\mathbf{J}_1^2} \\ & = \sum_{s_i \tilde{s}_i \tilde{t}_i \tilde{s}_i} \frac{1}{(2\pi)^3 A^+ B^-} \int d^4 J_1 d\bar{A}^+ \hat{\sigma}_{q\bar{q} \rightarrow \gamma^*}^{s_1, t_1; \tilde{s}_1, \tilde{t}_1; \mu_1}(\hat{s} = 2J_1^+ J_1^-) \hat{\sigma}_{q\bar{q} \rightarrow \gamma^*}^{s_2, t_2; \tilde{s}_2, \tilde{t}_2; \mu_2}(\hat{s} = 2J_2^+ J_2^-) \\ & \quad \times \left[ \frac{2}{(2\pi)^7} \sum_{\chi} \int \frac{d^2 \Delta}{(2\pi)^2} d^2 \bar{A} d\bar{A}^- d^2 \mathbf{a}_1 \psi_p^{s_1 s_2 \chi}(J_1^+, J_2^+, \mathbf{a}_1, \mathbf{a}_2, \bar{A}^-) \right] \tag{2.28} \\ & \quad \times \psi_p^{*\tilde{s}_1 \tilde{s}_2 \chi}(J_1^+, J_2^+, \mathbf{a}_1 + \Delta, \mathbf{a}_2 - \Delta, \bar{A}^-) J_1^+ J_2^+ A^+ \left] g_s^2 P_{g \rightarrow q\bar{q}}^{\lambda \rightarrow t_2 t_1, \tilde{t}_2 \tilde{t}_1} \left( \frac{J_2^-}{J_1^- + J_2^-} \right) \frac{1}{\mathbf{J}_1^2} \end{aligned}$$

In (2.28) we have once again introduced the transverse variable  $\Delta$  via the same relation as in the  $2v2$  case. We recognise the object in square brackets in (2.28) as the integral of the nonperturbatively generated parton pair  $\mathbf{r}$ -space 2pGPD over  $\Delta$ . If we make a change of longitudinal integration variables in (2.28) to the scaling variables (2.15), then we finally obtain:

$$\begin{aligned} \sigma_{2v1}(s) & = \sum_{s_i \tilde{s}_i \tilde{t}_i} \int dx_1 dx_2 dy_1 dy_2 \hat{\sigma}_{q\bar{q} \rightarrow \gamma^*}^{s_1, t_1; \tilde{s}_1, \tilde{t}_1; \mu_1}(\hat{s} = x_1 y_1 s) \hat{\sigma}_{q\bar{q} \rightarrow \gamma^*}^{s_2, t_2; \tilde{s}_2, \tilde{t}_2; \mu_2}(\hat{s} = x_2 y_2 s) \tag{2.29} \\ & \quad \times \left[ \int \frac{d^2 \Delta}{(2\pi)^2} \Gamma_{p; q\bar{q}}^{s_1 s_2, \tilde{s}_1 \tilde{s}_2}(x_1, x_2; \Delta) \right] \left[ \frac{\alpha_s}{2\pi} P_{g \rightarrow q\bar{q}}^{\lambda \rightarrow t_2 t_1, \tilde{t}_2 \tilde{t}_1}(y_2) \delta(1 - y_1 - y_2) \int_{\Lambda^2}^{Q^2} \frac{d\mathbf{J}_1^2}{\mathbf{J}_1^2} \right] \end{aligned}$$

We have restricted our integration over  $\mathbf{J}_1^2$  to the range  $\Lambda^2 < \mathbf{J}_1^2 < Q^2$ , which corresponds to the range over which our approximate expression for the matrix element

(2.25) is valid. The contributions to  $\sigma_{2v1}$  coming from  $\mathbf{J}_1^2$  values outside this range do not have the same  $1/\mathbf{J}_1^2$  structure.

The integral over  $\mathbf{J}_1$  in (2.29) gives rise to a large transverse momentum logarithm  $\log(Q^2/\Lambda^2)$ , whilst the integral over  $\Delta$  gives a prefactor of order  $\Lambda^2 \sim 1/R_p^2$  (since the nonperturbatively generated parton pair  $\mathbf{r}$ -space 2pGPD only has support for transverse momenta, and therefore transverse momentum imbalances  $\mathbf{r}$ , of order  $\Lambda_{QCD}$ ). Thus, as we asserted at the beginning of this section, there is a part of the cross section expression for figure 4(a) that is proportional to  $\log(Q^2/\Lambda^2)/R_p^2$  and should be included in the LO DPS cross section.

Note that the quantity  $\int d^2\Delta \Gamma_p^{s_1 s_2, \bar{s}_1 \bar{s}_2}(x_1, x_2; \Delta)/(2\pi)^2$  is equal to the  $\mathbf{b}$ -space nonperturbatively generated parton pair 2pGPD evaluated at zero transverse separation,  $\Gamma_p^{s_1 s_2, \bar{s}_1 \bar{s}_2}(x_1, x_2; \mathbf{b} = \mathbf{0})$ . This appears to indicate that the 2v1 contribution to DPS probes nonperturbatively generated parton pair 2pGPDs at zero parton separation. In fact, the result (2.29) actually corresponds to a broad logarithmic integral over values of  $\mathbf{b}^2$  that are  $\ll R_p^2$  but  $\gg 1/Q^2$ . The  $\mathbf{b}$ -space 2pGPD evaluated at  $\mathbf{b} = \mathbf{0}$  appears in (2.29) because the  $\mathbf{r}$ -space nonperturbatively generated parton pair 2pGPD dies off rapidly for  $\Delta^2 \gg \Lambda^2$ , which is equivalent to the  $\mathbf{b}$ -space nonperturbatively generated parton pair 2pGPD not containing any fluctuations with length scales  $\ll R_p$ . Then we can approximate  $\Gamma_p(\mathbf{b})$  for the relevant values of  $\mathbf{b}$  in (2.29) by  $\Gamma_p(\mathbf{b} = \mathbf{0})$ .

If one assumes that diagrams of the form of figure 1(b) are the only diagrams of the ‘2v1’ type that contribute to the DPS cross section at leading logarithmic order, then a generalisation of the result in (2.29) yields the expression below for the contribution of 2v1 graphs to the LO DPS cross section<sup>1</sup>:

$$\begin{aligned} \sigma_{(A,B)}^{D,2v1}(s) = & 2 \times \frac{m}{2} \sum_{i_1 j_1 i_2' j_2'} \int_{\Lambda^2}^{Q^2} dk^2 \frac{\alpha_s(k^2)}{2\pi k^2} \int dx_1 dx_2 dy_1 dy_2 \frac{dx_1'}{x_1'} \frac{dx_2'}{x_2'} \frac{dy_1'}{y_1'} \frac{dy_2'}{y_2'} \\ & \times \hat{\sigma}_{i_1 j_1 \rightarrow A}(\hat{s} = x_1 y_1 s) \hat{\sigma}_{i_2 j_2 \rightarrow B}(\hat{s} = x_2 y_2 s) \\ & \times \frac{D_p^l(y_1' + y_2', k^2)}{y_1' + y_2'} P_{l \rightarrow j_1' j_2'} \left( \frac{y_1'}{y_1' + y_2'} \right) D_{j_1'}^{j_1} \left( \frac{y_1}{y_1}; k^2, Q^2 \right) D_{j_2'}^{j_2} \left( \frac{y_2}{y_2}; k^2, Q^2 \right) \\ & \times D_{i_1'}^{i_1} \left( \frac{x_1}{x_1'}; \Lambda^2, Q^2 \right) D_{i_2'}^{i_2} \left( \frac{x_2}{x_2'}; \Lambda^2, Q^2 \right) \Gamma_{p, indep}^{i_1' i_2'}(x_1', x_2', \mathbf{b} = \mathbf{0}; \Lambda^2) \end{aligned} \quad (2.30)$$

$D_i^j(x; k^2, Q^2)$  are the Green’s functions of the DGLAP equations – i.e. a set of functions obeying the DGLAP equations with the initial condition  $D_i^j(x; k^2, k^2) = \delta_{ij} \delta(1-x)$ .  $\Gamma_{p, indep}^{i_1' i_2'}(x_1', x_2'; \mathbf{b} = \mathbf{0}, \Lambda^2)$  represents a nonperturbative initial condition for the two independent ladders in figure 1(b). In (2.30) we have re-inserted the symmetry factor  $m/2$  that

---

<sup>1</sup>Note that here and in the rest of this section we will take the scales associated with the two hard scales to be equal,  $Q_A^2 = Q_B^2 = Q^2$ . We will comment in section 4 on the generalisation of the results of this section to the case of unequal scales. Note also that we only write down the unpolarised diagonal contribution in colour, flavour and spin space here. The contributions associated with spin polarisation (either longitudinal or transverse) and flavour interference are expected to have a similar structure. On the other hand, it is known that the colour correlation/interference and parton type interference contributions will be suppressed by Sudakov factors, as is discussed in [5, 6, 26, 30].

has been omitted in earlier discussion in this section ( $m = 1$  if the two hard processes are identical, and  $m = 2$  otherwise). There is an additional prefactor of 2 in (2.30) because there are two sets of 2v1 graphs that give equivalent contributions – in one set the non-perturbatively generated parton pair emerges from the ‘left’ proton, whilst in the other it emerges from the ‘right’ proton.

Equation (2.30) can be written in a more compact fashion as:

$$\begin{aligned}
\sigma_{(A,B)}^{D,2v1}(s) &= 2 \times \frac{m}{2} \sum_{i_i j_i} \int dx_1 dx_2 dy_1 dy_2 \hat{\sigma}_{i_1 j_1 \rightarrow A}(\hat{s} = x_1 y_1 s) \hat{\sigma}_{i_2 j_2 \rightarrow B}(\hat{s} = x_2 y_2 s) \quad (2.31) \\
&\quad \times \check{D}_p^{j_1 j_2}(y_1, y_2; Q^2) \int \frac{d^2 \Delta}{(2\pi)^2} \Gamma_{p, indep}^{i_1 i_2}(x_1, x_2, \Delta; Q^2) \\
&= 2 \times \frac{m}{2} \sum_{i_i j_i} \int dx_1 dx_2 dy_1 dy_2 \hat{\sigma}_{i_1 j_1 \rightarrow A}(\hat{s} = x_1 y_1 s) \hat{\sigma}_{i_2 j_2 \rightarrow B}(\hat{s} = x_2 y_2 s) \\
&\quad \times \check{D}_p^{j_1 j_2}(y_1, y_2; Q^2) \Gamma_{p, indep}^{i_1 i_2}(x_1, x_2, \mathbf{b} = \mathbf{0}; Q^2)
\end{aligned}$$

where:

$$\Gamma_{p, indep}^{i_1 i_2}(x_1, x_2, \mathbf{b}; Q^2) \equiv \sum_{i'_i} \int \frac{dx'_1}{x'_1} \frac{dx'_2}{x'_2} D_{i'_1}^{i_1} \left( \frac{x_1}{x'_1}; \Lambda^2, Q^2 \right) D_{i'_2}^{i_2} \left( \frac{x_2}{x'_2}; \Lambda^2, Q^2 \right) \quad (2.32)$$

$$\begin{aligned}
&\quad \times \Gamma_{p, indep}^{i'_1 i'_2}(x'_1, x'_2, \mathbf{b}; \Lambda^2) \\
\check{D}_p^{j_1 j_2}(y_1, y_2; Q^2) &\equiv \sum_{l'_j} \int_{\Lambda^2}^{Q^2} dk^2 \frac{\alpha_s(k^2)}{2\pi k^2} \frac{dy'_1}{y'_1} \frac{dy'_2}{y'_2} \frac{D_p^l(y'_1 + y'_2, k^2)}{y'_1 + y'_2} \quad (2.33) \\
&\quad \times P_{l \rightarrow j'_1 j'_2} \left( \frac{y'_1}{y'_1 + y'_2} \right) D_{j'_1}^{j_1} \left( \frac{y_1}{y'_1}; k^2, Q^2 \right) D_{j'_2}^{j_2} \left( \frac{y_2}{y'_2}; k^2, Q^2 \right)
\end{aligned}$$

As mentioned in section 1, and as will be explored in detail in section 3, there are additional diagrams of the ‘2v1’ type that contribute at leading logarithmic order to the DPS cross section, aside from those represented by figure 1(b). These involve crosstalk interactions between the two nonperturbatively generated ladders. Equation (2.30) (or (2.31)) therefore represents only part of the 2v1 contribution to the LO DPS cross section. For the moment, however, we’ll limit our discussion to just this part.

A necessary requirement for (2.30) (or (2.31)) to be valid (at least as an incomplete part of a contribution to the DPS cross section) is that the independent two-ladder 2pGPD  $\Gamma_{p, indep}^{i_1 i_2}(x_1, x_2; \mathbf{b}, Q^2)$  should be smooth on distance scales  $\ll R_p \sim 1/\Lambda$  (or equivalently that the corresponding distribution in terms of the transverse momentum imbalance  $\Delta$  is cut off at values of order  $\Lambda$ ). This appears to be a somewhat reasonable requirement – at the scale  $\Lambda$  there is only this scale available to set the size of the  $\Delta$  profile for  $\Gamma_{p, indep}^{i_1 i_2}(x_1, x_2; \Delta, \Lambda^2)$ , and the evolution equation for the independent two-ladder 2pGPD (which is just the ‘double DGLAP’ equation of [21, 22] with the ‘single PDF feed term’ defined in [31] removed) preserves the transverse profile. In any case, such behaviour for  $\Gamma_{p, indep}^{i_1 i_2}(x_1, x_2; \Delta, Q^2)$  would appear to be required in order to get the necessary prefactor of order  $1/R_p^2$  in the 2v2 contribution to DPS, which is calculated according to the following

expression (for the diagonal unpolarised contribution):

$$\begin{aligned}
\sigma_{(A,B)}^{D,2v2}(s) &= \frac{m}{2} \sum_{i_i j_i} \int dx_1 dx_2 dy_1 dy_2 \hat{\sigma}_{i_1 j_1 \rightarrow A}(\hat{s} = x_1 y_1 s) \hat{\sigma}_{i_2 j_2 \rightarrow B}(\hat{s} = x_2 y_2 s) \\
&\quad \times \int \frac{d^2 \Delta}{(2\pi)^2} \Gamma_{p, indep}^{i_1 i_2}(x_1, x_2, \Delta; Q^2) \Gamma_{p, indep}^{j_1 j_2}(y_1, y_2, -\Delta; Q^2) \\
&= \frac{m}{2} \sum_{i_i j_i} \int dx_1 dx_2 dy_1 dy_2 \hat{\sigma}_{i_1 j_1 \rightarrow A}(\hat{s} = x_1 y_1 s) \hat{\sigma}_{i_2 j_2 \rightarrow B}(\hat{s} = x_2 y_2 s) \\
&\quad \times \int d^2 \mathbf{b} \Gamma_{p, indep}^{i_1 i_2}(x_1, x_2, \mathbf{b}; Q^2) \Gamma_{p, indep}^{j_1 j_2}(y_1, y_2, \mathbf{b}; Q^2)
\end{aligned} \tag{2.34}$$

If one assumes that  $\Gamma_{p, indep}^{ij}(x_1, x_2; \mathbf{b}, Q^2)$  can be factorised into a longitudinal piece  $\tilde{D}_{p, indep}^{ij}(x_1, x_2; Q^2)$  and a flavour-independent transverse piece  $F(\mathbf{b})$ , where  $F(\mathbf{b})$  is a smooth function of radius  $R_p$  normalised to 1, then (2.30) and (2.34) become:

$$\begin{aligned}
\sigma_{(A,B)}^{D,2v2}(s) &= \frac{m}{2} \sum_{i_i j_i} \frac{1}{\sigma_{eff,2v2}} \int dx_1 dx_2 dy_1 dy_2 \hat{\sigma}_{i_1 j_1 \rightarrow A}(\hat{s} = x_1 y_1 s) \\
&\quad \times \hat{\sigma}_{i_2 j_2 \rightarrow B}(\hat{s} = x_2 y_2 s) \tilde{D}_{p, indep}^{i_1 i_2}(x_1, x_2; Q^2) \tilde{D}_{p, indep}^{j_1 j_2}(y_1, y_2; Q^2)
\end{aligned} \tag{2.35}$$

$$\begin{aligned}
\sigma_{(A,B)}^{D,2v1}(s) &= 2 \times \frac{m}{2} \sum_{i_i j_i} \frac{1}{\sigma_{eff,2v1}} \int dx_1 dx_2 dy_1 dy_2 \hat{\sigma}_{i_1 j_1 \rightarrow A}(\hat{s} = x_1 y_1 s) \\
&\quad \times \hat{\sigma}_{i_2 j_2 \rightarrow B}(\hat{s} = x_2 y_2 s) \tilde{D}_p^{j_1 j_2}(y_1, y_2; Q^2) \tilde{D}_{p, indep}^{i_1 i_2}(x_1, x_2; Q^2)
\end{aligned} \tag{2.36}$$

where:

$$\frac{1}{\sigma_{eff,2v2}} \equiv \int d^2 \mathbf{b} [F(\mathbf{b})]^2 = \int \frac{d^2 \Delta}{(2\pi)^2} [F(\Delta)]^2 \tag{2.37}$$

$$\frac{1}{\sigma_{eff,2v1}} \equiv F(\mathbf{b} = \mathbf{0}) = \int \frac{d^2 \Delta}{(2\pi)^2} [F(\Delta)] \tag{2.38}$$

$F(\Delta)$  is the Fourier transform of  $F(\mathbf{b})$ . We see that the geometrical prefactors for the two different contributions to the DPS cross section are different in general,  $\sigma_{eff,2v2} \neq \sigma_{eff,2v1}$ . If one assumes that two nonperturbatively generated ladders are to some degree uncorrelated in transverse space,  $F(\mathbf{b})$  is given by a convolution of an azimuthally symmetric transverse parton density in the proton  $\rho(\mathbf{r})$  with itself, where  $\rho(\mathbf{r})$  must be normalised to 1 in order to ensure the appropriate normalisation of  $F(\mathbf{b})$ :

$$F(\mathbf{b}) = \int d^2 \mathbf{r} \rho(\mathbf{r}) \rho(\mathbf{b} - \mathbf{r}) \tag{2.39}$$

Then, if one takes the Gaussian form  $\exp[-r^2/(2R^2)]/(\pi R^2)$  for  $\rho$  (with  $R$  a constant parameter), one finds that  $\sigma_{eff,2v1} = \sigma_{eff,2v2}/2$  – that is, the 2v1 contribution receives a factor of 2 enhancement over the 2v2 contribution from the geometrical prefactor alone (in the next section, we'll discover that the 2v1 contribution is further enhanced at low  $x$  as a result of the crosstalk interactions on the two-ladder side that are allowed for this contribution). The ratio  $\sigma_{eff,2v2}/\sigma_{eff,2v1}$  does not depend much on the precise shape of  $\rho$

– for example, one obtains 2.18 if  $\rho$  is a top hat  $\frac{1}{\pi R^2}\Theta(R-r)$ , 2.32 if  $\rho$  is the projection of an exponential  $\int dz \frac{1}{8\pi R^3} \exp(\sqrt{-r^2+z^2}/R)$ , and 1.94 if  $\rho$  is the projection of a hard sphere  $\frac{3}{2\pi R^2}(1-r^2/R^2)^{1/2}\Theta(R-r)$  (with  $R$  once again a constant parameter in these expressions). This ‘factor of two’ enhancement of each 2v1 contribution over the 2v2 contribution from the geometrical prefactor has previously been noted in [19, 32]. It is important to bear in mind, however, that in order to obtain an enhancement that is roughly a factor of 2 one has to make a number of assumptions whose validity is somewhat uncertain (this is particularly the case for the assumption (2.39)). There could be some ‘clustering’ of the nonperturbative partons in transverse space, which would tend to increase  $\sigma_{eff,2v2}/\sigma_{eff,2v1}$ . Alternatively it is not inconceivable that the probability to find two nonperturbative partons separated by small distances  $\ll R_p$  could be smaller than the probability to find them separated by distances of order  $R_p$  – in this scenario  $\sigma_{eff,2v2}/\sigma_{eff,2v1}$  would be reduced.

### 3 Crosstalk between Ladders in the 2v1 Contribution

In the previous section we demonstrated that there is a leading logarithmic contribution to the DPS cross section associated with diagrams in which a single parton ladder from one proton splits into two, and then the two daughter ladders interact with two independent ladders from the other proton (that are only connected to one another via low-scale nonperturbative interactions). It is suggested in a number of works [19, 25, 33] that these diagrams are the only ones involving a single  $1 \rightarrow 2$  ladder branching that give rise to a leading logarithmic contribution to DPS. Here, we show that there is also a leading logarithmic contribution to the DPS cross section associated with diagrams such as those in figure 3 in which the two nonperturbatively generated ladders talk to one another by exchanging partons, provided that the crosstalk occurs at a lower scale than the scale of the  $1 \rightarrow 2$  ladder branching. There are two types of crosstalk that are possible, which are illustrated in the simple diagrams in figure 5(a) and (b) – we’ll call these off-diagonal real emission and virtual exchange processes respectively. As in the previous section, we’ll demonstrate that there is a leading logarithmic contribution from diagrams such as figure 3 by examining one of the simplest possible diagrams of the appropriate type – namely, that of figure 5(a). We will find that there is a large DGLAP logarithm associated with both the  $1 \rightarrow 2$  splitting and the off-diagonal real emission (‘crosstalk’) processes in the figure, and that this is associated exclusively with the region of integration in which the partonic products of the off-diagonal real emission have much smaller transverse momentum than the products of the  $1 \rightarrow 2$  splitting (and all of these transverse momenta are  $\gg \Lambda^2$  but  $\ll Q^2$ ).

In our calculation, we’ll ignore considerations of colour for simplicity, just as we did in section 2. However, the colour structure of crosstalk processes is quite nontrivial, and is important when considering the size of such contributions to cross sections. The colour structure of crosstalk processes has been considered previously in the context of twist-4 contributions to DIS in [34–37], and in the context of DPS in [24, 26, 38]. We will make some comments with regards to the colour structure of the crosstalk processes at the end of this section.

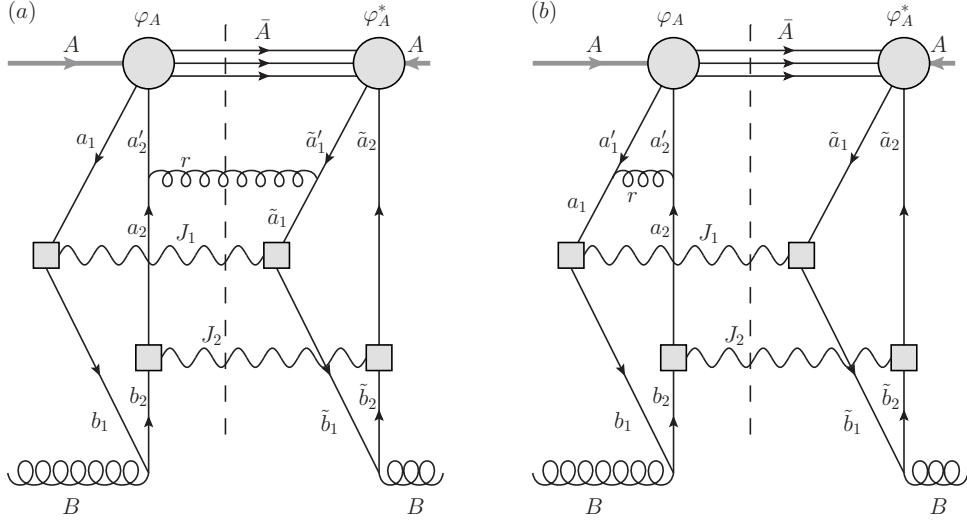


**Figure 5.** (a) Simple 2v1 diagram including an ‘off-diagonal real emission’ process. (b) Simple 2v1 diagram including a ‘virtual exchange’ process.

As in section 2, we work in a frame in which  $A = A^+p, B = B^-n$ . The cross section expression associated with figure 5(a) is:

$$\sigma_{XT}(s) = \frac{1}{2(2\pi)^{10}s} \int d^4\bar{A}d^4rd^4J_1d^4J_2\delta(J_1^2 - Q^2)\delta(J_2^2 - Q^2)\delta(r^2) \quad (3.1)$$

$$\delta^{(4)}(A + B - \bar{A} - r - J_1 - J_2)\mathcal{M}_L^{\lambda_1;\mu_1\mu_2\mu_3\chi}(A, B; J_1, J_2, r, \bar{A})$$

$$\mathcal{M}_R^{\lambda_1;\mu_1\mu_2\mu_3\chi}(A, B; J_1, J_2, r, \bar{A})^*$$

where:

$$\mathcal{M}_L^{\lambda_1;\mu_1\mu_2\mu_3\chi}(A, B; J_1, J_2, r, \bar{A}) \quad (3.2)$$

$$= i^9 g_s^2 (eQ_q)^2 \int \frac{d^4a_1}{(2\pi)^4} \frac{\text{Tr} \left[ \not{\epsilon}_{\lambda_1}(B) \not{b}_1 \not{\epsilon}_{\mu_1}^*(J_1) \not{a}_1 \not{\epsilon}_{\mu_2}^{\chi}(a_1, a_2, \bar{A}) \not{a}_2 \not{\epsilon}_{\mu_3}^*(r) \not{a}_2 \not{\epsilon}_{\mu_2}^*(J_2) \not{b}_2 \right]}{D(a_1)D(b_1)D(a_2)D(b_2)D(a_2)}$$

$$\mathcal{M}_R^{\lambda_1;\mu_1\mu_2\mu_3\chi}(A, B; J_1, J_2, r, \bar{A}) \quad (3.3)$$

$$= i^9 g_s^2 (eQ_q)^2 \int \frac{d^4\tilde{a}_1}{(2\pi)^4} \frac{\text{Tr} \left[ \not{\epsilon}_{\lambda_1}(B) \not{\tilde{b}}_1 \not{\epsilon}_{\mu_1}^*(J_1) \not{\tilde{a}}_1 \not{\epsilon}_{\mu_3}^*(r) \not{\tilde{a}}_1 \not{\epsilon}_{\mu_2}^{\chi}(\tilde{a}_1, \tilde{a}_2, \bar{A}) \not{\tilde{a}}_2 \not{\epsilon}_{\mu_2}^*(J_2) \not{\tilde{b}}_2 \right]}{D(\tilde{a}_1)D(\tilde{b}_1)D(\tilde{a}_1)D(\tilde{b}_2)D(\tilde{a}_2)}$$

Following a procedure that is similar to that leading to equation (2.22), and is valid in the region of transverse momentum integration in which  $\mathbf{J}_1^2, \mathbf{J}_2^2, r^2 \gg \Lambda^2$  (or equivalently

$\mathbf{a}_2^2, \mathbf{b}_1^2, \mathbf{b}_2^2 \gg \Lambda^2$ ), we can write down the following approximate expression for  $\mathcal{M}_L$ :

$$\begin{aligned}
& \mathcal{M}_L^{\lambda; \mu_1 \mu_2 \mu_3 \chi}(A, B; J_1, J_2, r, \bar{A}) \tag{3.4} \\
& \simeq \sum_{s_1 s'_2} \int \frac{da_1^+}{2\pi} \left[ \int d^2 \mathbf{a}_1 / (2\pi)^2 \psi_p^{s_1 s'_2 \chi}(a_1^+, a_2^{'+}, \mathbf{a}_1, \mathbf{a}'_2, \bar{A}^-) \right] \\
& \quad \times \frac{\mathcal{T}_L^{s'_2 s_1 \lambda; \mu_1 \mu_2 \mu_3}(a'_2 a_1 B \rightarrow J_1 J_2 r)|_{a_1^- = 0, \mathbf{a}_1 = 0}}{[2(J_1^+ - a_1^+) J_1^- - \mathbf{J}_1^2 + i\epsilon][2(a_1^+ - J_1^+)(B^- - J_1^-) - \mathbf{J}_1^2 + i\epsilon]} \\
& \quad \times \frac{1}{[2(J_1^+ + J_2^+ - a_1^+)(-r^-) - \mathbf{r}^2 + i\epsilon]}
\end{aligned}$$

where  $\mathcal{T}_L(a_2 a_1 B \rightarrow J_1 J_2 r)$  includes all of the numerator structure of the  $\mathcal{M}_L(a_2 a_1 B \rightarrow J_1 J_2 r)$  matrix element.

Performing the  $a_1^+$  integral using contour methods, and making use of the fact that the overall integrand is strongly peaked near  $a_1^+ = J_1^+$  whilst the numerator factor  $\mathcal{T}_L$  is a relatively smooth function in this region, we obtain:

$$\begin{aligned}
& \mathcal{M}_L^{\lambda; \mu_1 \mu_2 \mu_3 \chi}(A, B; J_1, J_2, r, \bar{A}) \tag{3.5} \\
& \simeq \sum_{s_1 s'_2} \frac{-ir^+}{2} \left[ \int d^2 \mathbf{a}_1 / (2\pi)^2 \psi_p^{s_1 s'_2 \chi}(J_1^+, a_2^{'+}, \mathbf{a}_1, \mathbf{a}'_2, \bar{A}^-) \right] \\
& \quad \times \frac{\mathcal{T}_L^{s'_2 s_1 \lambda; \mu_1 \mu_2 \mu_3}(a'_2 a_1 B \rightarrow J_1 J_2 r)|_{a_1^+ = J_1^+, a_1^- = 0, \mathbf{a}_1 = 0}}{\mathbf{J}_1^2 \mathbf{r}^2 [J_2^+ + \frac{\mathbf{J}_1^2}{2J_1^-} + r^+]}
\end{aligned}$$

In the region of integration in which  $\mathbf{J}_1^2 \ll Q^2$ , we can drop the second term in the denominator factor  $[J_2^+ + \frac{\mathbf{J}_1^2}{2J_1^-} + r^+]$ . Also, when  $\mathbf{J}_1^2, \mathbf{J}_2^2, \mathbf{r}^2 \ll Q^2$ , we can approximately decompose  $\mathcal{T}_L$  as follows:

$$\begin{aligned}
& \mathcal{T}_L^{s'_2 s_1 \lambda; \mu_1 \mu_2 \mu_3}(a'_2 a_1 B \rightarrow J_1 J_2 r)|_{a_1^- = 0, \mathbf{a}_1 = 0} \simeq \mathcal{M}_{q\bar{q} \rightarrow \gamma^*}^{s_1 t_1; \mu_1}(J_1^+ p, J_1^- n \rightarrow J_1) \tag{3.6} \\
& \quad \times \mathcal{M}_{\bar{q}q \rightarrow \gamma^*}^{s_2 t_2; \mu_2}(J_2^+ p, J_2^- n \rightarrow J_2) \mathcal{M}_{\bar{q} \rightarrow \bar{q}g}^{s'_2 \rightarrow s_2 \mu_3}(a_2^{'+} p, a_2^+ p - \mathbf{r}, (a_2^{'+} - a_2^+) p + \mathbf{r}) \\
& \quad \times \mathcal{M}_{g \rightarrow \bar{q}q}^{\lambda \rightarrow t_1 t_2}(B; J_1^- n + \mathbf{J}_1, J_2^- n - \mathbf{J}_1)
\end{aligned}$$

Performing a similar sequence of operations for  $\mathcal{M}_R$ , we obtain the expression below that is valid for  $\Lambda^2 \ll \tilde{\mathbf{a}}_1^2, \tilde{\mathbf{b}}_1^2, \tilde{\mathbf{b}}_2^2 \ll Q^2$ , or equivalently  $\Lambda^2 \ll \mathbf{J}_1^2, \mathbf{J}_2^2, \mathbf{r}^2 \ll Q^2$ :

$$\begin{aligned}
& \mathcal{M}_R^{\lambda; \mu_1 \mu_2 \mu_3 \chi}(A, B; J_1, J_2, r, \bar{A}) \tag{3.7} \\
& \simeq \sum_{s_i} \frac{-ir^+}{2} \left[ \int d^2 \tilde{\mathbf{a}}_1 / (2\pi)^2 \psi_p^{\tilde{s}'_1 \tilde{s}_2 \chi}(\tilde{a}_1^{'+}, J_2^+, \tilde{\mathbf{a}}'_1, \tilde{\mathbf{a}}_2, \bar{A}^-) \right] \\
& \quad \times \frac{\mathcal{M}_{q \rightarrow qg}^{\tilde{s}'_1 \rightarrow \tilde{s}_1 \mu_3}(\tilde{a}_1^{'+} p, a_1^+ p - \mathbf{r}, (\tilde{a}_1^{'+} - a_1^+) p + \mathbf{r})}{\mathbf{J}_2^2 \mathbf{r}^2 [J_1^+ + \frac{\mathbf{J}_2^2}{2J_2^-} + r^+]} \\
& \quad \times \mathcal{M}_{q\bar{q} \rightarrow \gamma^*}^{\tilde{s}_1 \tilde{t}_1; \mu_1}(J_1^+ p, J_1^- n \rightarrow J_1) \mathcal{M}_{\bar{q}q \rightarrow \gamma^*}^{\tilde{s}_2 \tilde{t}_2; \mu_2}(J_2^+ p, J_2^- n \rightarrow J_2) \\
& \quad \times \mathcal{M}_{g \rightarrow \bar{q}q}^{\lambda \rightarrow \tilde{t}_1 \tilde{t}_2}(B; J_1^- n - \mathbf{J}_2, J_2^- n + \mathbf{J}_2)
\end{aligned}$$

Given that the transverse momenta of the partons emerging from the  $g \rightarrow q\bar{q}$  branching process are different on the left and right hand sides of the cut in figure 5(a) ( $\pm\mathbf{J}_1$  and  $\mp\mathbf{J}_2$  respectively), we will require a generalised version of the relation (2.26), which reads:

$$\begin{aligned} & \frac{J_1^- J_2^-}{(J_1^- + J_2^-)^2} \mathcal{M}_{g \rightarrow q\bar{q}}^{\lambda \rightarrow t_1 t_2}(B; J_1^- n + \mathbf{J}_1, J_2^- n - \mathbf{J}_1) \mathcal{M}_{g \rightarrow q\bar{q}}^{*\lambda \rightarrow \tilde{t}_1 \tilde{t}_2}(B; J_1^- n - \mathbf{J}_2, J_2^- n + \mathbf{J}_2) \quad (3.8) \\ & = -4g_s^2 P_{g \rightarrow q\bar{q}}^{\lambda \rightarrow t_2 t_1, \tilde{t}_2 \tilde{t}_1} \left( \frac{J_2^-}{J_1^- + J_2^-} \right) \epsilon_\lambda \cdot \mathbf{J}_1 \epsilon_\lambda^* \cdot \mathbf{J}_2 \end{aligned}$$

Note that in the off-diagonal emission process, the partons emitting the gluon in the amplitude and conjugate do not in general have the same plus momentum (and indeed are not of the same type). This means that the product of  $\mathcal{M}_{\bar{q} \rightarrow qg}$  and  $\mathcal{M}_{q \rightarrow qg}^*$  from the left and right hand sides of the diagram does not give rise to a conventional splitting function multiplied by the appropriate transverse momentum squared, as occurred in (2.26). Instead, one obtains:

$$\begin{aligned} & \frac{r^+ A^+}{\tilde{a}_1^+ a_2^+} \sqrt{\frac{a_1^+ a_2^+}{\tilde{a}_1^+ a_2^+}} \mathcal{M}_{\bar{q} \rightarrow qg}^{s_2' \rightarrow s_2 \mu_3}(a_2^+ p, a_2^+ p - \mathbf{r}, (a_2^+ - a_2^+) p + \mathbf{r}) \quad (3.9) \\ & \quad \times \mathcal{M}_{q \rightarrow qg}^{*\tilde{s}_1' \rightarrow \tilde{s}_1 \mu_3}(\tilde{a}_1^+ p, a_1^+ p - \mathbf{r}, (\tilde{a}_1^+ - a_1^+) p + \mathbf{r}) \\ & \quad \equiv 2g_s^2 V_{I, q \rightarrow q}^{\tilde{s}_1' s_2' \rightarrow \tilde{s}_1 s_2; \mu_3} \left( \frac{a_1^+}{A^+}, \frac{\tilde{a}_1^+}{A^+}, \frac{a_2^+}{A^+} \right) \mathbf{r}^2 \end{aligned}$$

where  $V_{I, q \rightarrow q}^{\tilde{s}_1' s_2' \rightarrow \tilde{s}_1 s_2; \mu_3} \left( \frac{a_1^+}{A^+}, \frac{\tilde{a}_1^+}{A^+}, \frac{a_2^+}{A^+} \right)$  represents some kind of generalised splitting function, that satisfies the following relation:

$$V_{I, q \rightarrow q}^{\tilde{s}_1' s_2' \rightarrow \tilde{s}_1 s_2; \mu_3} \left( \frac{a^+}{A^+}, \frac{a'^+}{A^+}, \frac{a'^+}{A^+} \right) = \frac{A^+}{a'^+} P_{q\bar{q}}^{\tilde{s}_1' s_2' \rightarrow \tilde{s}_1 s_2; \mu_3} \left( \frac{a^+}{a'^+} \right) \quad (3.10)$$

Furthermore, since the partons emerging from the hadronic blob in figure 5(a) do not in general carry the same momentum on the left and right hand sides of the diagram, the process in figure 5(a) probes a two-parton PDF that is not diagonal in  $x$ . It is defined according to:

$$\begin{aligned} & \Gamma_{p; q\bar{q}}^{s_1 s_2, \tilde{s}_1 \tilde{s}_2} \left( \frac{a_1^+}{A^+}, \frac{a_2'^+}{A^+}, \frac{\tilde{a}_1'^+}{A^+} \right) \equiv \frac{2}{(2\pi)^9} \sum_\chi \int d\bar{A}^- d^2 \bar{\mathbf{A}} d^2 \mathbf{a}_1 d^2 \tilde{\mathbf{a}}_1' \sqrt{a_1^+ a_2'^+ \tilde{a}_1'^+ \tilde{a}_2'^+} A^+ \quad (3.11) \\ & \quad \times \psi_{p; q\bar{q}}^{s_1 s_2 \chi}(a_1^+, a_2'^+, \mathbf{a}_1, \mathbf{a}_2', \bar{A}^-, \bar{\mathbf{A}}) \psi_{p; q\bar{q}}^{*s_1' s_2' \chi}(\tilde{a}_1'^+, \tilde{a}_2'^+, \tilde{\mathbf{a}}_1', \tilde{\mathbf{a}}_2', \bar{A}^-, \bar{\mathbf{A}}) \end{aligned}$$

Note that this distribution is somewhat similar to the four-quark matrix element that is probed in the twist-four contribution to Drell-Yan, and that is defined in [39–42]. Here, however, we do not absorb two powers of the strong coupling constant  $g_s$  into the four quark matrix element, as is done (and makes sense) in the context of the twist-four contribution to Drell-Yan.

Inserting (3.5), (3.6), and (3.7) into (3.1), and making use of (3.8), (3.9) and (3.11), we find that the contribution to  $\sigma_{XT}$  coming from the region of transverse momentum

integration with  $\Lambda^2 \ll \mathbf{r}^2, \mathbf{J}_1^2, \mathbf{J}_2^2 \ll Q^2$  is:

$$\begin{aligned} \sigma_{XT}(s) = & \sum_{s_i \tilde{s}_i t_i \tilde{t}_i s'_1 s'_2} \int dx_1 dx_2 dy_1 dy_2 \hat{\sigma}_{q\bar{q} \rightarrow \gamma^*}^{s_1, t_1; \tilde{s}_1, \tilde{t}_1; \mu_1}(\hat{s} = x_1 y_1 s) \hat{\sigma}_{q\bar{q} \rightarrow \gamma^*}^{s_2, t_2; \tilde{s}_2, \tilde{t}_2; \mu_2}(\hat{s} = x_2 y_2 s) \\ & \left[ \frac{\alpha_s}{2\pi} \int_{x_1}^{1-x_2} d\tilde{x}'_1 V_{I, q \rightarrow q}^{\tilde{s}'_1 s'_2 \rightarrow \tilde{s}_1 s_2; \mu_3}(x_1, \tilde{x}'_1, x'_2) \Gamma_{p; q\bar{q}}^{s_1 s'_2, \tilde{s}'_1 \tilde{s}_2}(x_1, x'_2, \tilde{x}'_1) \right] \\ & \left[ \frac{\alpha_s}{2\pi} P_{g \rightarrow q\bar{q}}^{\lambda \rightarrow t_2 t_1, \tilde{t}_2 \tilde{t}_1}(y_2) \delta(1 - y_1 - y_2) \right] \int d\mathbf{J}_1^2 d\mathbf{r}^2 \frac{2\epsilon_\lambda \cdot \mathbf{J}_1 \epsilon_\lambda^* \cdot (\mathbf{J}_1 + \mathbf{r})}{r^2 \mathbf{J}_1^2 (\mathbf{J}_1 + \mathbf{r})^2} \end{aligned} \quad (3.12)$$

In the region of transverse momentum integration in which  $\mathbf{r}^2 \ll \mathbf{J}_1^2, \mathbf{J}_2^2$ , the transverse momentum integrand simplifies as below, and we obtain two large DGLAP logarithms from this region:

$$\int d\mathbf{J}_1^2 d\mathbf{r}^2 \frac{2\epsilon_\lambda \cdot \mathbf{J}_1 \epsilon_\lambda^* \cdot (\mathbf{J}_1 + \mathbf{r})}{r^2 \mathbf{J}_1^2 (\mathbf{J}_1 + \mathbf{r})^2} \xrightarrow{\mathbf{J}_1^2 \gg \mathbf{r}^2} \int_{\Lambda^2}^{Q^2} \frac{d\mathbf{J}_1^2}{\mathbf{J}_1^2} \int_{\Lambda^2}^{\mathbf{J}_1^2} \frac{d\mathbf{r}^2}{\mathbf{r}^2} = \log^2 \left( \frac{Q^2}{\Lambda^2} \right) \quad (3.13)$$

Two large DGLAP logarithms implies a leading logarithmic contribution, since there are two powers of  $\alpha_s$  in (3.12). Thus, there is a leading logarithmic contribution to the DPS cross section coming from the region of figure 5(a) in which  $\mathbf{r}^2 \ll \mathbf{J}_1^2$  (i.e. in which the scale of the off-diagonal real emission process is strictly smaller than the scale of the  $1 \rightarrow 2$  branching process). It is only this region of transverse momentum integration that gives rise to a leading double logarithm – other regions only give rise to either a single logarithm, or no logarithm at all. The single DGLAP logarithm is essentially associated with a logarithmic integral over  $\mathbf{r}$  only, and this should be absorbed into the four-quark matrix element in the ‘conventional’ twist-4 contribution to double Drell-Yan.

In (3.12) we have not explicitly written the scales associated with the two factors of  $\alpha_s$ . It should be clear that in the integration region that gives rise to the leading logarithm, the appropriate scale for the first  $\alpha_s$  factor should be  $\mathbf{r}^2$ , whilst that for the second factor should be  $\mathbf{J}_1^2$  (with  $\mathbf{r}^2 \ll \mathbf{J}_1^2$  in the integration region of interest). This is because the first coupling constant is associated with the crosstalk interaction (that gives rise to transverse parton momenta of order  $\mathbf{r}^2$ ), whilst the second is associated with the  $1 \rightarrow 2$  splitting (that gives rise to transverse parton momenta of order  $\mathbf{J}_1^2$ ).

Aside from the process in figure 5(a) involving an off-diagonal real emission, the process in figure 5(b) involving a virtual exchange also gives rise to a leading double logarithm, provided once again that the virtual exchange process occurs at a lower scale than the  $1 \rightarrow 2$  branching. This is straightforward to show using a procedure similar to the one we have used above. Generalising these results, we find that in the most general 2v1 DPS diagram, all possible types of parton exchange are allowed inside the two ladders emerging from one of the protons at leading logarithmic order, provided that they occur at a lower scale than the  $1 \rightarrow 2$  ladder branching occurring in the other proton. Schematically, the

LO (diagonal unpolarised) cross section expression for the 2v1 contribution to DPS is:

$$\begin{aligned}
\sigma_{(A,B)}^{D,2v1}(s) = & 2 \times \frac{m}{2} \sum_{li_j i' i'_i} \int_{\Lambda^2}^{Q^2} dk^2 \frac{\alpha_s(k^2)}{2\pi k^2} \int dx_1 dx_2 dy_1 dy_2 \frac{dx'_1}{x'_1} \frac{dx'_2}{x'_2} \frac{dy'_1}{y'_1} \frac{dy'_2}{y'_2} \\
& \times \hat{\sigma}_{i_1 j_1 \rightarrow A}(\hat{s} = x_1 y_1 s) \hat{\sigma}_{i_2 j_2 \rightarrow B}(\hat{s} = x_2 y_2 s) \\
& \times \frac{D_p^l(y'_1 + y'_2, k^2)}{y'_1 + y'_2} P_{l \rightarrow j'_1 j'_2} \left( \frac{y'_1}{y'_1 + y'_2} \right) D_{j'_1}^{j_1} \left( \frac{y_1}{y'_1}; k^2, Q^2 \right) D_{j'_2}^{j_2} \left( \frac{y_2}{y'_2}; k^2, Q^2 \right) \\
& \times D_{i'_1}^{i_1} \left( \frac{x_1}{x'_1}; k^2, Q^2 \right) D_{i'_2}^{i_2} \left( \frac{x_2}{x'_2}; k^2, Q^2 \right) \Gamma_p^{i'_1 i'_2}(x'_1, x'_2; x'_1, k^2)
\end{aligned} \tag{3.14}$$

$\Gamma_p^{i'_1 i'_2}(x_1, x_2; \tilde{x}_1, \mu^2)$  is a four-parton matrix element whose evolution involves all possible exchanges between these partons in an axial gauge – i.e. the two types of real emission plus virtual exchange and self energy corrections<sup>2</sup>. Taking Mellin moments of this function gives rise to a matrix element of one of the so-called ‘quasiparton operators’ whose evolution is discussed in [43]. Note that taking Mellin moments of a 2pGPD normally does not give rise to the expectation value of a quasiparton operator, due to the finite  $\mathbf{b}$ .

It is straightforward to show that if the crosstalk interactions are omitted, then equation (3.14) reduces to (2.30). With crosstalk interactions absent,  $\Gamma_p^{i'_1 i'_2}(x'_1, x'_2; x'_1, k^2)$  in (3.14) is built up from two independent ladders:

$$\Gamma_p^{i'_1 i'_2}(x'_1, x'_2; x'_1, k^2) = \Gamma_{p, indep}^{i'_1 i'_2}(x'_1, x'_2, \mathbf{b} = \mathbf{0}; k^2) \tag{3.15}$$

where  $\Gamma_{p, indep}^{i'_1 i'_2}$  is given by (2.32). Substituting this expression for  $\Gamma_p^{i'_1 i'_2}(x'_1, x'_2; x'_1, k^2)$  into (3.14), and making use of the relation:

$$\sum_j \int_x^1 \frac{dx'}{x'} D_i^j(x'; \Lambda^2, k^2) D_j^k \left( \frac{x}{x'}; k^2, Q^2 \right) = D_i^k(x; \Lambda^2, Q^2) \tag{3.16}$$

we observe that the expression for  $\sigma_{(A,B)}^{D,2v1}$  becomes equal to (2.30).

At the next-to-leading logarithmic (or NLO) level, one would need to append an extra term to (3.14) that is of the following form:

$$\int dx_1 dx_2 d\tilde{x}_1 dy D_p^k(y, Q^2) \Gamma_p^{ij}(x_1, x_2; \tilde{x}_1, Q^2) \hat{\sigma}_{ijk \rightarrow AB}(x_1, x_2, \tilde{x}_1, y) \tag{3.17}$$

This is essentially the ‘conventional’ twist-4 contribution to the  $pp \rightarrow AB + X$  production cross section. At the level of total cross sections, the DPS contribution to the production of  $AB$  cannot be distinguished from the conventional twist-4 contribution, and the two should really just be considered together as components of the  $\mathcal{O}(\Lambda^2/Q^2)$  correction to the  $pp \rightarrow AB + X$  cross section.

Let us now discuss the issue of colour in the evolution of the four-parton (twist-4) matrix element  $\Gamma_p^{i'_1 i'_2}(x_1, x_2; \tilde{x}_1, \mu^2)$ . We recall that, for the 2pGPD with finite  $\mathbf{b}$ , every

---

<sup>2</sup>In a covariant gauge, such as Feynman gauge, there are further diagrams that contribute to the evolution due to the presence of a nontrivial Wilson line in the definition of the operator. These diagrams involve gluon connections to the Wilson line.

distribution that does not have the partons with the same light-cone momentum fractions on either side of the cut paired up into colour singlets is suppressed by a Sudakov factor – see [5, 6, 26, 30]. This factor arises in axial gauge because there is an incomplete cancellation of the soft gluon region between (diagonal) real emission diagrams and virtual self-energy corrections in the colour interference/correlation distributions [30]. In physical terms, it occurs because such distributions involve a movement of colour by the large transverse distance  $\mathbf{b}$  in the hadron [26].

In the twist-4 matrix element  $\Gamma_p^{i_1' i_2'}(x_1, x_2; \tilde{x}_1, \mu^2)$  there is no such Sudakov suppression of colour interference/correlation distributions. The extra diagrams that are allowed in the evolution of this distribution (i.e. the off-diagonal emission and virtual exchange diagrams in axial gauge) provide extra soft-gluon divergences that cancel any remaining divergence from adding the diagonal real emission and virtual self-energy diagrams together. The soft divergence in both real emission diagrams (diagonal and off-diagonal) is positive, whilst that in both virtual diagrams (self-energy and exchange) is negative, and in the sum the positive and negative contributions always cancel each other out. We can see why this cancellation occurs physically as follows. In the operator definition of the twist-4 matrix element, the four operators corresponding to the partons all lie on the same lightlike line, with no transverse separation between any of them. Note that this does not exactly correspond to the physical situation that we have in the 2v1 graphs – in these, the transverse separation of the partons in the nonperturbatively generated pair must be equal to that of the partons emerging from the  $1 \rightarrow 2$  splitting in the other proton, which is of order  $1/k$  (with  $k^2$  equal to the scale of the  $1 \rightarrow 2$  splitting). However, for the purposes of obtaining  $\Gamma_p^{i_1' i_2'}(x_1', x_2'; x_1', k^2)$  in (3.14) by solving the evolution equation at scales  $\mu^2 < k^2$ , this separation is not resolvable and effectively can be taken as zero. The fact that the four operators/partons in  $\Gamma_p^{i_1' i_2'}(x_1, x_2; \tilde{x}_1, \mu^2)$  are on top of (or at least very close to) one another in transverse space means that soft longwave gluons can only resolve the total colour of all of them. But the summed colour of the four partons must be zero, since the proton is a colour singlet object – therefore the effects of soft gluons must cancel, as is indeed observed in practical calculations. The cancellation of soft gluon divergences in the twist-4 matrix elements has been discussed before, in [34, 44, 45] (for example).

It is important to point out that we are not claiming here that colour interference contributions to the 2v1 DPS cross section are free from Sudakov suppression. Rather, we are stating the well-known theoretical fact that there can be no Sudakov suppression in any twist-4 matrix element. In the 2v1 DPS cross section there can be a Sudakov suppression if the partons coming from either proton are not colour matched between amplitude and conjugate at scales  $\mu^2 > k^2$  at which the parton transverse separation  $\sim 1/k^2$  is resolvable. On the two initial-state ladder side, and at scales  $\mu^2 < k^2$  at which the parton transverse separation is not resolvable, the way in which colour is distributed between the parton legs in amplitude and conjugate can change with no accompanying Sudakov suppression.

Let us now consider the region of small  $x$  in the four-parton matrix element (which one might believe to be the most relevant region for DPS at the LHC – but see later). It is well known that in this region the gluons dominate, so we will only consider these partons in

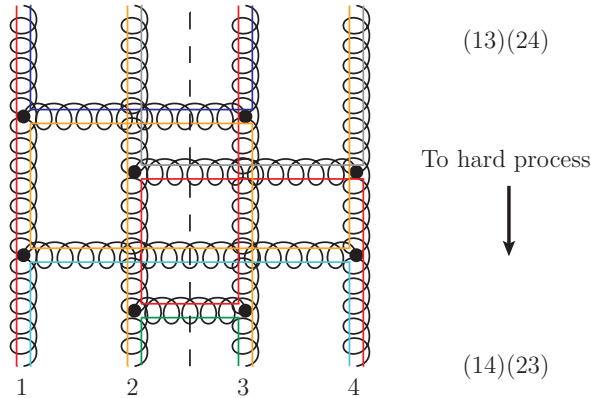


**Figure 6.** A process that can bring about a colour recombination in the four gluon state. On the diagram we have indicated the colour flow in the large  $N_C$  limit.

what follows. We have seen that the colour correlated/interference twist-4 distributions are not Sudakov suppressed – however, in the low  $x$  region, the distributions in which two pairs of gluons are in colour singlet configurations tend to win out. This is because the colour factors in the anomalous dimensions for these distributions are larger (see section 3.2 of [34] or section 5.1.3 of [6]). Bear in mind that in figure 3 at scale  $k^2$  the nonperturbatively generated partons with identical  $x$  fractions must be in a colour singlet state if one wants to avoid any Sudakov suppression. By combining two off-diagonal real emission processes put together with two diagonal real emission processes as in figure 6, it is possible to achieve a ‘colour recombination’ on the two ladder side at scales lower than  $k^2$ , and alter the way in which the parton legs are grouped into two sets of colour singlets. For example, in figure 6 the grouping is changed from (14)(23) afterwards to (13)(24) before, using the leg labelling conventions from the figure. Such a colour recombination is not disfavoured from the point of view of evolution before and after the process – however, it is itself suppressed by a colour factor equal to  $1/(N_C^2 - 1)$  [34–38]. This colour factor suppression is associated with the fact that the recombination process is non-planar.

From the point of view of low  $x$  physics, there is an important distinction between the two crosstalk processes that we have discussed in this section – i.e. the off-diagonal real emission and virtual exchange processes. The off-diagonal real emission process can significantly reduce the magnitudes of the lightcone momentum fractions of the two active parton legs involved in the process, since it is a real emission process. On the other hand, the same is not true for the virtual exchange process. Here, the sum of the lightcone momentum fractions of the two parton legs involved must be conserved, and since the two legs are forced to have positive lightcone momentum fractions by the kinematics of the process, the magnitudes of both  $x$ s cannot simultaneously decrease – one must increase to compensate the decrease of the other. This means that, taking all partons involved to be gluons as is appropriate at low  $x$ , the virtual exchange splitting function is not enhanced at small  $x$  in the same way that the off-diagonal exchange (and indeed diagonal exchange) splitting functions are. In particular, the virtual exchange diagrams do not contribute at

double leading logarithmic order to the evolution of the four-gluon matrix element. This result has been known for some time – see [34, 46–50]. This is the reason why we drew the colour recombination process in figure 6 using two off-diagonal real emission processes – it would be also possible to engineer a colour recombination using two virtual exchange processes instead, but such a process would not be as strongly enhanced at low  $x$ .

We now discuss the important question of the numerical impact of the crosstalk interactions on the 2v1 DPS cross section. A complete investigation of this issue at leading logarithmic order in QCD would require taking into consideration all partonic, spin and colour channels, and the calculation and numerical implementation of all of the evolution kernels between these channels at leading order. This is beyond the scope of this paper – however, we can make a few important comments.

One might expect the effects of the crosstalk interactions to be negligible based on the colour suppression of these interactions in the twist-4 matrix element that we mentioned above. On the other hand, in [37], an investigation into the size of crosstalk effects in the four-gluon matrix element was performed using the double leading logarithmic approximation (and in the context of shadowing corrections to DIS), and it was found that the size of the effects is appreciable even for not too small  $x$  and evolution lengths. It was shown that the effects of the crosstalk interactions on the four-gluon matrix element could be approximately described by the following ‘K-factor’ (here we include the effects of the running coupling):

$$K_{BR}(Y, \xi) = 1 + 2\sqrt{\pi\delta} \left( \frac{4N_C}{\pi b} Y \ln \left( \frac{\xi - \xi_\Lambda}{-\xi_\Lambda} \right) \right)^{1/4} \quad (3.18)$$

where  $\delta \sim 1/N_C^4$ ,  $b = (33 - 2N_f)/(12\pi)$ ,  $Y = \ln(1/x)$ ,  $\xi = \ln(Q^2/Q_0^2)$ ,  $\xi_\Lambda = \ln(\Lambda_{QCD}^2/Q_0^2)$ ,  $Q_0^2$  is the scale at which one begins including crosstalk effects,  $Q^2$  is the final scale, and  $x$  corresponds to the size of the  $x$  values in the matrix element. If one plugs the sample values  $x = 0.001$ ,  $Q = 5$  GeV,  $Q_0 = 1$  GeV,  $\Lambda_{QCD} = 0.359$  GeV,  $N_f = 3$  into this formula, one obtains  $K_{BR} = 1.96$  - a significant enhancement despite the  $1/(N_C^2 - 1)$  suppression of the recombination vertex. Thus, we cannot simply ignore recombination processes in the 2v1 DPS cross section based only on their colour suppression.

An important point to emphasise in the context of numerical considerations is that the 2v1 contribution to DPS does not probe the twist-4 matrix elements at  $\mu^2 = Q^2$  and  $x \sim x_h$  (where  $x_h$  represents the values of  $x$  associated with the hard scatterings). Rather, the twist-4 matrix elements are probed at  $\mu^2 = k^2$  and  $x = x_{sp}$ , where  $x_{sp}$  is the  $x$  value appropriate to the  $1 \rightarrow 2$  splitting. In general we will have  $k^2 < Q^2$ ,  $x_{sp} > x_h$ , which gives a smaller ‘evolution space’ in  $x$  and  $\mu^2$  for the crosstalk effects, and a smaller enhancement.

Of course, there will not be a single value of  $k^2$  and  $x_{sp}$  that applies to all 2v1 graphs that have a particular hard scale  $Q^2$  and particular values of  $x$  at that hard scale – instead we integrate over  $k^2$  and  $x_{sp}$ , as one can see from looking at the equation (3.14) ( $x_{sp} = y'_1 + y'_2$  in this equation). Two factors determine the average values of  $Y_{split}$  and  $\xi_{split}$  in a particular set of 2v1 graphs – the first is that we have two ladders rather than one after the split on the one ladder side (which will tend to prefer smaller  $Y_{split}$  and  $\xi_{split}$ ), and the second is that we have no crosstalk interactions after the split on the two ladder side

(which will tend to prefer larger  $Y_{split}$  and  $\xi_{split}$ ). One expects the first effect to be strongly dominant, in which case we can estimate  $\langle Y_{split} \rangle$  and  $\langle \xi_{split} \rangle$  for particular final  $x$  and  $Q^2$  values by considering just the one-ladder side. For example, we can estimate  $\langle Y_{split} \rangle(x, Q^2)$  by weighting the integral (2.33) by  $\ln(1/(y'_1 + y'_2))$ , setting  $y_1 \simeq y_2 \simeq x$ , and then dividing by  $\check{D}_p(x, x; Q^2)$ .

Using this method, we estimated the values of  $\langle Y_{split} \rangle$  and  $\langle \xi_{split} \rangle$  for various values of  $x$  at the hard interaction, and for  $Q = 10$  GeV. In our approximate calculation we included only gluons, taking as input the MSTW2008LO gluon input at  $Q_0 = 1$  GeV (and only integrating  $k^2$  down to  $Q_0^2$  in (2.33) and the weighted integral). The number of flavours was held fixed,  $N_f = 3$ , we take  $\Lambda_{QCD} = 0.359$  GeV, and we used the full  $g \rightarrow g$  splitting functions.

The results of this calculation are given in table 1. Rather than  $\langle Y_{split} \rangle$  and  $\langle \xi_{split} \rangle$ , we have chosen to tabulate the values of  $x$  and  $\mu^2$  corresponding to these values – i.e.  $\exp(-\langle Y_{split} \rangle)$  and  $Q_0 \sqrt{\exp(\langle \xi_{split} \rangle)}$  respectively. We also tabulate the values of  $K_{BR}$  corresponding to each set of  $(\langle Y_{split} \rangle, \langle \xi_{split} \rangle)$  values.

One notices immediately from the table that the  $x$  values of splitting are much larger than that at the hard process, and the  $Q$  values of splitting tend to be rather close to  $Q_0$  (as was also noticed in [33]). For  $x \gtrsim 10^{-3}$ , the  $x$  values at the splitting begin to enter the region  $\gtrsim 10^{-1}$  in which PDFs decrease with  $\mu^2$  rather than increase (as the dominant process becomes splitting to smaller  $x$  values rather than the ‘feed’ from larger  $x$  values). For such  $x$  values, the net effect of including crosstalk interactions should either be small, or should actually be to reduce the 2v1 cross section (as the crosstalk interactions offer extra pathways by which the four-gluon matrix element can decrease rather than increase). Clearly, we cannot place any trust at all in the  $K_{BR}$  values quoted in table 1 for  $x \gtrsim 10^{-3}$ .

For much smaller  $x$  values (e.g.  $10^{-6}$ ) the  $x$  values at the splitting are smaller (although not by much), and one might anticipate an enhancement of the 2v1 cross section due to crosstalk interactions, although perhaps not as large as the formula (3.18) predicts. One must bear in mind, however, that for such small  $x$  values the DGLAP approach we have taken here may not be so well justified, and an alternative approach based on the BFKL equation may be more appropriate.

Note that the results we obtained were for  $Q = 10$  GeV. The  $x$  and  $\mu^2$  values corresponding to  $\langle Y_{split} \rangle$  and  $\langle \xi_{split} \rangle$  are plotted against  $Q^2$  for various values of  $x$  in figure 7. We notice that the typical  $x$  and  $\mu^2$  values of splitting increase with  $Q^2$ , although beyond  $Q = 10$  GeV the typical  $x$  values do not increase by much, and one would expect the conclusions we have found above to also hold for larger  $Q$  values.

Thus, we have provided an indication that for not too small  $x$  values ( $\gtrsim 10^{-3}$ ), crosstalk interactions should not significantly enhance the cross section, and indeed they most likely reduce it. Moderate  $x$  values ( $10^{-3} - 10^{-2}$ ) correspond to  $x_{sp}$  values  $\simeq 0.1$  where PDFs do not change significantly with scale, so one might expect the effect of crosstalk effects on the DPS cross section to be small at such  $x$  values – however, a more complete numerical investigation, which is beyond the scope of this paper, is required to make a more definite statement.

The statement that the ‘ $\mathbf{b} = \mathbf{0}$ ’ twist-4 distributions probed in the 2v1 contribution

$x$	$\exp(-\langle Y_{split} \rangle)$	$Q_0 \sqrt{\exp(\langle \xi_{split} \rangle)}$	$K_{BR}(\langle Y_{split} \rangle, \langle \xi_{split} \rangle)$
1.0E-06	4.5E-02	1.34	1.56
3.6E-05	6.4E-02	1.44	1.57
1.3E-03	9.1E-02	1.67	1.59
4.6E-02	2.1E-01	2.35	1.59
9.9E-02	3.1E-01	2.67	1.56

**Table 1.** Average  $Y$  and  $\xi$  values of the  $1 \rightarrow 2$  splitting for a ‘perturbatively generated’ pair of partons with the  $x$  values in the table, and probed at  $Q = 10$  GeV. Note that we have actually tabulated the  $x$  and  $\mu^2$  values corresponding to these average  $Y$  and  $\xi$  values. The values of  $K_{BR}$  corresponding to the average  $Y$  and  $\xi$  values are tabulated, but for reasons given in the text one should not place much trust in these figures.

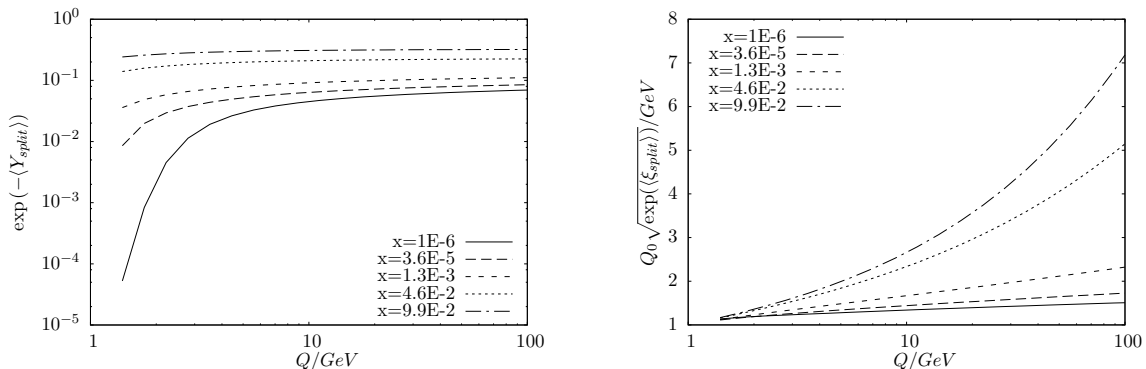


**Figure 7.** Plots showing the  $x$  and  $\mu^2$  values corresponding to the average  $Y$  and  $\xi$  values of the  $1 \rightarrow 2$  splitting, plotted against  $Q^2$ , and for various values of  $x$  at the hard interaction.

to DPS evolve differently from the 2pGPDs with finite  $\mathbf{b}$  has been made recently in Appendix A of [24]. However, in this paper it is claimed that only the evolution of the colour correlation/interference distributions changes at  $\mathbf{b} = \mathbf{0}$  – we contend that the evolution of the colour diagonal/singlet distribution is also affected in an important way. In equation (A1) of [24], an evolution equation for the colour octet twist-4  $q\bar{q}$  distribution diagonal in  $x$  fractions is proposed. However, the equation they propose involves only similar distributions diagonal in  $x$  fractions on the right hand side – in fact the correct evolution equation should contain more general distributions nondiagonal in  $x$  on the right hand side, since the crosstalk processes that are allowed for  $\mathbf{b} = \mathbf{0}$  will necessarily disrupt a diagonal/symmetric pattern of  $x$  values.

#### 4 The Total Cross Section for Double Parton Scattering

In a previous publication [20] (see also [51]), we examined another class of diagrams that can contribute to the DPS cross section – the ‘1v1’ graphs. For the arbitrary ‘1v1’ graph in figure 1(c) with a total of  $n$  QCD branching vertices in the amplitude or conjugate, we discovered that there is no natural piece of the diagram that is proportional to  $\log(Q^2/\Lambda^2)^n/R_p^2$  and is associated with the transverse momenta inside the loop being strongly ordered on

either side of the diagram (in fact, most of the contribution to the total cross section expression for the graph comes from the region of integration in which the transverse momenta of particles inside the loop are of  $\mathcal{O}(\sqrt{Q^2})$ ). Based on this finding, we suggested that 1v1 graphs should not contribute to the pp DPS cross section.

Combining this suggestion with the findings of sections 2 and 3, we obtain the following formula for the total DPS cross section:

$$\sigma_{(A,B)}^D(s) = \sigma_{(A,B)}^{D,2v2}(s) + \sigma_{(A,B)}^{D,2v1}(s) \quad (4.1)$$

with  $\sigma_{(A,B)}^{D,2v2}(s)$  and  $\sigma_{(A,B)}^{D,2v1}(s)$  being given by the expressions (2.34) and (3.14) respectively<sup>3</sup>.

This formula agrees with the DPS cross section formulae proposed in [24, 26] and [19], apart from the fact that in neither of these papers are the crosstalk effects in the 2v1 graphs taken into account correctly (in [19] they are omitted, whilst in [24, 26] they are included in an incorrect fashion). Ryskin and Snigirev [25] include an extra ‘1v1’ contribution in their proposed cross section formula, which they argue can be validly included in the DPS cross section at suitably low  $x$  [33], but which should not be included at moderate to large  $x$  values.

We would like to point out at this stage that there are two features in the equation (4.1) that are potentially concerning, and that might indicate that modifications to it may be required in order to correctly describe the DPS cross section.

The first issue is that we were originally expecting to obtain an expression for the DPS cross section looking something like (1.1), with the 2pGPDs in these formulae each having an interpretation in terms of hadronic operator matrix elements. Our proposed expression (4.1) deviates somewhat in structure from these expectations.

The second issue is that there is a rather sharp distinction in (4.1) between perturbatively and nonperturbatively generated parton pairs, with the 2pGPD for the latter having a natural width in  $\mathbf{r}$  space of order  $\Lambda$  (as was discussed in section 2). Does there exist some scale at which we can (approximately) regard all parton pairs in the proton as being ‘nonperturbatively generated’ in this sense (as is assumed in (4.1))? If so, what is the appropriate value for the scale (presumably it should be rather close to  $\Lambda_{QCD}$ )?

These issues are related in an essential way to the fact that we have cut the contribution from ‘1v1’ graphs out of the DPS cross section entirely. It may therefore not be correct to entirely remove these graphs from the DPS cross section in this way. On the other hand, at present we do not have a suitable alternative prescription for handling these graphs, and leave finding the appropriate way of including the 1v1 graphs to future work.

---

<sup>3</sup>Note that this is really our prediction for the unpolarised diagonal contribution to the total DPS cross section when the scales of the two hard interactions are the same,  $Q_A^2 = Q_B^2 = Q^2$ . To generalise this result to unequal scales, one needs to change  $Q^2$  to  $Q_A^2$  in all Green’s functions in (3.14) involving a ‘1’ index, change  $Q^2$  to  $Q_B^2$  in all Green’s functions in (3.14) involving a ‘2’ index, change the upper limit of the  $k^2$  integration to  $\min(Q_A^2, Q_B^2)$ , and perform a similar operation for the ‘2v2’ contribution. As mentioned previously, the contributions associated with spin polarisation (either longitudinal or transverse) and flavour interference are expected to have a similar structure to (4.1), whilst the colour correlation/interference and parton type interference contributions should be suppressed by Sudakov factors, as is discussed in [5, 6, 26, 30].

## 5 Conclusions

In this paper we have closely examined the contribution to the LO p-p DPS cross section from graphs in which two ‘nonperturbatively generated’ ladders interact with two ladders that have been generated via a perturbative  $1 \rightarrow 2$  branching process – ‘2v1’ graphs. We have presented a detailed calculation demonstrating that 2v1 graphs in which the two nonperturbatively generated ladders do not interact with one another contribute to the LO p-p DPS cross section in the way originally written down by Ryskin and Snigirev [25], and then later by Blok et al. [19] and Manohar and Waalewijn [24, 26]. We have also shown that 2v1 graphs in which the ‘nonperturbatively generated’ ladders exchange partons with one another contribute to the LO p-p DPS cross section, provided that this ‘crosstalk’ occurs at a lower scale than the  $1 \rightarrow 2$  branching on the other side of the graph. We have proposed a formula for the contribution from 2v1 graphs to the LO DPS cross section, equation (3.14).

Crosstalk interactions between the two nonperturbatively generated ladders are suppressed by colour effects – for example, the ‘colour recombination’ of figure 6 is suppressed by a factor  $1/(N_C^2 - 1)$ . This fact on it’s own does not necessarily mean that the effect of crosstalk interactions in the 2v1 diagrams is negligible. It was discovered in [37] that crosstalk interactions could lead to a sizeable increase in the cross section, even for rather small evolution lengths  $\ln(Q^2/Q_0^2) \simeq 3$  and for not too small ‘final’  $x$  values for the crosstalk  $\simeq 10^{-3}$ . However, we pointed out that in the 2v1 diagrams, the typical  $x$  values at which the  $1 \rightarrow 2$  splitting occurs, and the crosstalk finishes, are very much larger than those at the hard scale, and the  $\mu^2$  value of the splitting is much smaller than  $Q^2$ . For  $Q = 10$  GeV,  $x$  values at the hard scale  $\gtrsim 10^{-3}$  correspond to  $x$  values at the splitting  $\gtrsim 0.1$ , which is the region where PDFs either do not change, or decrease with scale. In this region of  $x$  the effect of crosstalk will either be small, or will be to decrease the cross section. We obtain very similar conclusions when moving to larger values of  $Q^2$ . Thus, except at exceedingly small  $x$  values, we expect the effects of crosstalk interactions to be a reduction of the 2v1 DPS cross section, which should be rather small at moderate  $x$  values  $\simeq 10^{-3} - 10^{-2}$  corresponding to  $x$  values at the splitting  $\simeq 0.1$ . A more precise statement than this requires a detailed numerical simulation of the 2v1 graphs, which is beyond the scope of this paper.

We combined our formula for the 2v1 contribution to the DPS cross section (3.14) with the suggestion that we made in [20] that 1v1 graphs should be completely removed from the DPS cross section to suggest a formula for the DPS cross section, equation (4.1). Two potentially concerning features were identified in this equation, and the existence of these might indicate that completely removing the 1v1 graphs from the DPS cross section is not quite the correct prescription. The determination of the appropriate manner of treating the 1v1 graphs is left to future work.

### Note Added

After this paper was completed we learned of the published version of ‘What is Double Parton Scattering?’ by Manohar and Waalewijn [52] in which were corrected the errors of

the original arXiv version [24] that we discussed at the end of section 3. The discussion in that paper now appears to be in alignment with our own findings.

## Acknowledgements

We gratefully acknowledge discussions with J. Stirling, and financial support from a Trinity College Senior Rouse Ball Studentship. All the figures in this paper were generated using JaxoDraw [53].

## References

- [1] A. Del Fabbro and D. Treleani, *A double parton scattering background to Higgs boson production at the LHC*, *Phys. Rev.* **D61** (2000) 077502, [[hep-ph/9911358](#)].
- [2] M. Y. Hussein, *A double parton scattering background to associate WH and ZH production at the LHC*, *Nucl. Phys. Proc. Suppl.* **174** (2007) 55–58, [[hep-ph/0610207](#)].
- [3] M. Y. Hussein, *Double parton scattering in associate Higgs boson production with bottom quarks at hadron colliders*, [arXiv:0710.0203](#).
- [4] D. Bandurin, G. Golovanov, and N. Skachkov, *Double parton interactions as a background to associated HW production at the Tevatron*, *JHEP* **1104** (2011) 054, [[arXiv:1011.2186](#)].
- [5] M. Diehl and A. Schafer, *Theoretical considerations on multiparton interactions in QCD*, *Phys.Lett.* **B698** (2011) 389–402, [[arXiv:1102.3081](#)].
- [6] M. Diehl, D. Ostermeier, and A. Schafer, *Elements of a theory for multiparton interactions in QCD*, *JHEP* **1203** (2012) 089, [[arXiv:1111.0910](#)].
- [7] **Axial Field Spectrometer** Collaboration, T. Akesson *et. al.*, *Double parton scattering in pp collisions at  $\sqrt{s} = 63\text{GeV}$* , *Z. Phys.* **C34** (1987) 163.
- [8] **UA2** Collaboration, J. Alitti *et. al.*, *A Study of multi - jet events at the CERN anti-p p collider and a search for double parton scattering*, *Phys.Lett.* **B268** (1991) 145–154.
- [9] **CDF** Collaboration, F. Abe *et. al.*, *Study of four jet events and evidence for double parton interactions in  $p\bar{p}$  collisions at  $\sqrt{s} = 1.8\text{TeV}$* , *Phys.Rev.* **D47** (1993) 4857–4871.
- [10] **CDF** Collaboration, F. Abe *et. al.*, *Double parton scattering in  $p\bar{p}$  collisions at  $\sqrt{s} = 1.8\text{TeV}$* , *Phys. Rev.* **D56** (1997) 3811–3832.
- [11] **D0** Collaboration, V. M. Abazov *et. al.*, *Double parton interactions in photon+3 jet events in p p- bar collisions sqrts=1.96 TeV*, *Phys. Rev.* **D81** (2010) 052012, [[arXiv:0912.5104](#)].
- [12] *A measurement of hard double-partonic interactions in  $W \rightarrow l\nu + 2\text{ jet events}$* , Tech. Rep. ATLAS-CONF-2011-160, CERN, Geneva, Dec, 2011.
- [13] P. Bartalini (ed.) and L. Fano (ed.), *Multiple partonic interactions at the LHC. Proceedings, 1st International Workshop, MPI'08, Perugia, Italy, October 27-31, 2008*, [arXiv:1003.4220](#).
- [14] <http://mpi10.desy.de/>.
- [15] <http://www.mpi2010.physics.gla.ac.uk/Home.html>.
- [16] <http://mpi11.desy.de/>.
- [17] P. Bartalini, E. Berger, B. Blok, G. Calucci, R. Corke, *et. al.*, *Multi-Parton Interactions at the LHC*, [arXiv:1111.0469](#).

- [18] B. Blok, Y. Dokshitzer, L. Frankfurt, and M. Strikman, *The Four jet production at LHC and Tevatron in QCD*, *Phys.Rev.* **D83** (2011) 071501, [[arXiv:1009.2714](#)].
- [19] B. Blok, Y. Dokshitzer, L. Frankfurt, and M. Strikman, *pQCD physics of multiparton interactions*, *Eur.Phys.J.* **C72** (2012) 1963, [[arXiv:1106.5533](#)].
- [20] J. R. Gaunt and W. J. Stirling, *Double Parton Scattering Singularity in One-Loop Integrals*, *JHEP* **1106** (2011) 048, [[arXiv:1103.1888](#)].
- [21] V. P. Shelest, A. M. Snigirev, and G. M. Zinovjev, *Gazing into the multiparton distribution equations in QCD*, *Phys. Lett.* **B113** (1982) 325.
- [22] G. M. Zinovev, A. M. Snigirev, and V. P. Shelest, *Equations for many parton distributions in quantum chromodynamics*, *Theor. Math. Phys.* **51** (1982) 523–528.
- [23] A. M. Snigirev, *Double parton distributions in the leading logarithm approximation of perturbative QCD*, *Phys. Rev.* **D68** (2003) 114012, [[hep-ph/0304172](#)].
- [24] A. V. Manohar and W. J. Waalewijn, *What is Double Parton Scattering?*, [arXiv:1202.5034v1](#).
- [25] M. Ryskin and A. Snigirev, *A Fresh look at double parton scattering*, *Phys.Rev.* **D83** (2011) 114047, [[arXiv:1103.3495](#)].
- [26] A. V. Manohar and W. J. Waalewijn, *A QCD Analysis of Double Parton Scattering: Color Correlations, Interference Effects and Evolution*, [arXiv:1202.3794](#). 24 pages, 15 figures.
- [27] N. Paver and D. Treleani, *Multi-quark scattering and large  $p_T$  jet production in hadronic collisions*, *Nuovo Cim.* **A70** (1982) 215.
- [28] M. Mekhfi, *Multiparton processes: an application to double Drell- Yan*, *Phys. Rev.* **D32** (1985) 2371.
- [29] M. E. Peskin and D. V. Schroeder, *An Introduction to quantum field theory*. Addison-Wesley Publishing Co., 1995.
- [30] M. Mekhfi and X. Artru, *Sudakov suppression of color correlations in multiparton scattering*, *Phys.Rev.* **D37** (1988) 2618–2622.
- [31] J. R. Gaunt and W. J. Stirling, *Double Parton Distributions Incorporating Perturbative QCD Evolution and Momentum and Quark Number Sum Rules*, *JHEP* **1003** (2010) 005, [[0910.4347](#)].
- [32] B. Blok, Y. Dokshitzer, L. Frankfurt, and M. Strikman, *Origins of Parton Correlations in Nucleon and Multi-Parton Collisions*, [arXiv:1206.5594](#).
- [33] M. Ryskin and A. Snigirev, *Double parton scattering in double logarithm approximation of perturbative QCD*, *Phys.Rev.* **D86** (2012) 014018, [[arXiv:1203.2330](#)].
- [34] E. Levin, M. Ryskin, and A. Shuvaev, *Anomalous dimension of the twist four gluon operator and pomeron cuts in deep inelastic scattering*, *Nucl.Phys.* **B387** (1992) 589–616.
- [35] J. Bartels, *Unitarity corrections to the Lipatov pomeron and the small  $x$  region in deep inelastic scattering in QCD*, *Phys.Lett.* **B298** (1993) 204–210.
- [36] J. Bartels, *Unitarity corrections to the Lipatov pomeron and the four gluon operator in deep inelastic scattering in QCD*, *Z.Phys.* **C60** (1993) 471–488.
- [37] J. Bartels and M. Ryskin, *Absorptive corrections to structure functions at small  $x$* , *Z.Phys.* **C60** (1993) 751–756.

- [38] J. Bartels and M. Ryskin, *Recombination within multi-chain contributions in pp scattering*, [arXiv:1105.1638](#).
- [39] R. K. Ellis, W. Furmanski, and R. Petronzio, *Power Corrections to the Parton Model in QCD*, *Nucl.Phys.* **B207** (1982) 1.
- [40] R. K. Ellis, W. Furmanski, and R. Petronzio, *Unraveling Higher Twists*, *Nucl.Phys.* **B212** (1983) 29.
- [41] J.-W. Qiu, *Twist four contributions to the parton structure functions*, *Phys.Rev.* **D42** (1990) 30–44.
- [42] J.-W. Qiu and G. F. Sterman, *Power corrections in hadronic scattering. 1. Leading  $1/Q^2$  corrections to the Drell-Yan cross-section*, *Nucl.Phys.* **B353** (1991) 105–136.
- [43] A. Bukhvostov, G. Frolov, L. Lipatov, and E. Kuraev, *Evolution Equations for Quasi-Partonic Operators*, *Nucl.Phys.* **B258** (1985) 601–646.
- [44] L. Gribov and M. Ryskin. LNPI-865 (1983).
- [45] L. Gribov, Y. Dokshitzer, S. Troyan, and V. Khoze *Sov. Phys. JETP* **88** (1988) 1303.
- [46] B. M. McCoy and T. T. Wu, *Mandelstam Diagrams Are Not Enough*, *Phys.Rev.* **D12** (1975) 546.
- [47] B. M. McCoy and T. T. Wu, *Three Particle Regge Pole in  $\phi^3$  Theory*, *Phys.Rev.* **D12** (1975) 578.
- [48] S. Matinyan and A. Sedrakyan *JETP Lett.* **23** (1976) 588.
- [49] S. Matinyan and A. Sedrakyan *JETP Lett.* **24** (1976) 240.
- [50] S. Matinyan and A. Sedrakyan *Sov. J. Nucl. Phys.* **24** (1976) 844.
- [51] J. R. Gaunt and W. J. Stirling, *Single and Double Perturbative Splitting Diagrams in Double Parton Scattering*, [arXiv:1202.3056](#).
- [52] A. V. Manohar and W. J. Waalewijn, *What is Double Parton Scattering?*, *Phys.Lett.* **B713** (2012) 196–201, [[arXiv:1202.5034v2](#)].
- [53] D. Binosi and L. Theußl, *JaxoDraw: A graphical user interface for drawing Feynman diagrams*, *Computer Physics Communications* **161** (2004) 76–86.